

2016

## Application of Time-Frequency Analysis to Characterize Gas Shadows from the Clinton interval in Ohio Seismic Reflection Data

Fangzhou Yan  
*Wright State University*

Follow this and additional works at: [https://corescholar.libraries.wright.edu/etd\\_all](https://corescholar.libraries.wright.edu/etd_all)



Part of the [Earth Sciences Commons](#), and the [Environmental Sciences Commons](#)

---

### Repository Citation

Yan, Fangzhou, "Application of Time-Frequency Analysis to Characterize Gas Shadows from the Clinton interval in Ohio Seismic Reflection Data" (2016). *Browse all Theses and Dissertations*. 1676.  
[https://corescholar.libraries.wright.edu/etd\\_all/1676](https://corescholar.libraries.wright.edu/etd_all/1676)

This Thesis is brought to you for free and open access by the Theses and Dissertations at CORE Scholar. It has been accepted for inclusion in Browse all Theses and Dissertations by an authorized administrator of CORE Scholar. For more information, please contact [library-corescholar@wright.edu](mailto:library-corescholar@wright.edu).

APPLICATION OF TIME-FREQUENCY ANALYSIS TO CHARACTERIZE GAS  
SHADOWS FROM THE CLINTON INTERVAL IN OHIO SEISMIC REFLECTION  
DATA

A thesis submitted in partial fulfillment of the requirements for the degree of  
Master of Science

By

FANGZHOU YAN

B.E., Taiyuan University of Technology, China, 2012

2016

Wright State University

WRIGHT STATE UNIVERSITY  
GRADUATE SCHOOL

Dec.7<sup>th</sup> 2016

I HEREBY RECOMMEND THAT THE THESIS PREPARED UNDER MY SUPERVISION  
BY FANGZHOU YAN ENTITLED Application of Time-Frequency Analysis to Characterize  
Gas Shadows from the Clinton interval in Ohio Seismic Reflection Data BE ACCEPTED IN  
PARTIAL FULFILLMENT OF THE REQUIREMENTS FOR THE DEGREE OF Master of  
Science.

---

Doyle R. Watts, Ph.D.  
Thesis Director

---

David F. Dominic, Ph.D.  
Chair, Department of Earth &  
Environmental Sciences

Committee on  
Final Examination

---

Doyle R. Watts, Ph.D.

---

Ernest C. Hauser, Ph. D.

---

David F. Dominic, Ph. D.

---

Robert E. W. Fyffe, Ph.D.  
Vice President for Research and  
Dean of the Graduate School

## **ABSTRACT**

Yan, Fangzhou. M.S. Department of Earth & Environment Sciences, Wright State University, 2016. Application of Time-Frequency Analysis to Characterize Gas Shadows from the Clinton interval in Ohio Seismic Reflection Data.

The Smoothed Pseudo Wigner-Ville Distribution (SPWVD) is one method to simultaneously resolve time series in both time and frequency domains, allowing determination of frequency variation with time in non-stationary signals. Also, SPWVD reduces the cross-term interference. This analysis was applied to stacked, migrated seismic reflection data from Ohio to characterize gas shadows produced by known and potential gas reservoirs in the Clinton interval. In northeast Ohio, the Clinton interval is identified as occurring immediately beneath the Dayton Limestone, which is known as the driller's Packer Shell in the subsurface.

The analysis was first applied to a seismic reflection line acquired from the East Dominion Ohio Gas Storage field that contained an example of a gas shadow. This analysis demonstrated that all frequencies were attenuated at otherwise continuous reflectors immediately beneath a portion of the Clinton interval fully charged with natural gas. There was no enhancement of low frequencies such as described in low frequency shadows from the Gulf of Mexico.

This analysis was applied to other seismic lines acquired in areas where natural gas is produced from the Clinton interval and areas of possible natural gas attenuation were identified. In this work, low frequencies are not enhanced beneath the potential gas



reservoir. To be successful, this method requires that continuous reflectors occur beneath the target horizon. Simple attenuation of signal from a continuous reflector may be a new direct indicator of natural gas on seismic reflection data from Ohio and other Paleozoic basins.

## Contents

1 Introduction.....	1
1.1 Gas Shadow.....	1
1.2 Time-Frequency Analysis .....	2
1.3 Hydrocarbon Production History in the Clinton interval in Ohio.....	4
1.4 Objective. ....	5
2 Geology.....	7
2.1 The Clinton interval .....	7
2.2 Previous Study of the Clinton interval .....	7
3 Method.....	11
3.1 Time-Frequency Characterization of a known Ohio Gas Shadow.....	11
3.2 Seismic reflection data from Muskingum County .....	12
3.2 Identification of reflectors using Well Logs .....	19
3.3 Wavelet Extraction and Synthetic Traces .....	19
3.4 Tie the synthetic trace to the seismogram.....	23
4 Results.....	27
4.1 Initial Production Map .....	27
4.2 Results of Time-Frequency Analysis .....	29
5 Summary & Discussion .....	54
6 References.....	57

## Table of Figures

FIGURE 1. MAP SHOWING LOCATION OF THE “THE CLINTON INTERVAL” OIL AND GAS FIELDS IN OHIO (GEOFACETS, JUNE 2015, OHIO DEPARTMENT OF NATURAL RESOURCES). THE GAS STORAGE FIELD AND MUSKINGUM COUNTY ARE MARKED AS TWO RED BOXES.....	6
FIGURE 2. SIMPLIFIED LITHOSTRATIGRAPHIC UNITS OF THE CLINTON INTERVAL AND VICINITY ( GEOFACETS,JUNE 2015, OHIO DEPARTMENT OF NATURAL RESOURCES). ....	8
FIGURE 3. SEISMIC LINE FROM GABOR GAS STORAGE FIELD SHOWING THE GAS SHADOW (AFTER HANEBERG-DIGGS, 2014). THE PACKER SHELL AND TOP CINCINNATI GROUP REFLECTORS ARE INDICATED. THE RED BOX INDICATES AN ATTENUATION ZONE DUE TO GAS SHADOW EFFECT.....	13
FIGURE 4. A 10 HZ COMMON FREQUENCY SECTION. THE RED BOX INDICATES THE ATTENUATION ZONE (GAS SHADOW) CENTERED AT 520MS (TOP OF THE CINCINNATI GROUP) FROM CDP4202 TO CDP 4219 .....	14
FIGURE 5. A 20 HZ COMMON FREQUENCY SECTION. THE RED LINE INDICATES THE ATTENUATION ZONE (GAS SHADOW) CENTERED AT 520MS (TOP OF THE CINCINNATI GROUP) FROM CDP4202 TO CDP 4219 .....	15
FIGURE 6. A 30 HZ COMMON FREQUENCY SECTION. THE RED LINE INDICATES THE ATTENUATION ZONE (GAS SHADOW) CENTERED AT 520MS (TOP OF THE CINCINNATI GROUP) FROM CDP4202 TO CDP 4212 .....	16
FIGURE 7. INSTANTANEOUS FREQUENCY AT THE MAXIMUM PHASE OF THE REFLECTOR CORRESPONDING TO THE TOP OF THE CINCINNATI GROUP AS INDICATED IN FIGURE 3	17
FIGURE 8. LOCATION OF SEISMIC LINES IN MUSKINGUM COUNTY. ....	18

FIGURE 9. DIGITIZED WELL #34119277010000 DENSITY LOG, SONIC LOG, GAMMA LOG WITH DRILLER'S TOPS.....	20
FIGURE 10. THE COMPUTED REFLECTIVITY LOG AND ACOUSTIC IMPEDENCE LOGS ASSOCIATED WITH FIGURE 9.....	22
FIGURE 11. UPPER FIGURE: THE EXTRACTION OF THE WAVELET CENTERED BETWEEN 300 MS AND 800 MS FROM LINE 5. LOWER FIGURE: EXTRACTED WAVELET AMPLITUDE AND FREQUENCY CONTENT. ....	23
FIGURE 12. THE BLACK TRACES ARE SYNTHETIC TRACES ASSOCIATED WITH THE WAVELET IN FIGURE 11. ....	25
FIGURE 13. LINE 5 TIED TO THE SYTHETIC TRACES. THE BIG LIME, PACKER SHELL AND TRENTON REFLECTORS ARE PICKED.....	26
FIGURE 14. INITIAL PRODUCTION MAP OF CLINTON GAS WELLS IN MUSKINGUM COUNTY WITH SEISMIC LINES AND WELL LOCATIONS. THE RED BOXES HIGHLIGHT HIGH GAS PRODUCTION ZONES. ....	28
FIGURE 15. A 10 HZ COMMON FREQUENCY SECTION OF LINE1. THE RED OVAL INDICATES THE ATTENUATION ZONE (GAS SHADOW) CENTERED AT THE TOP OF THE CINCINNATI GROUP REFLECTOR.....	30
FIGURE 16. A 20 HZ COMMON FREQUENCY SECTION OF LINE1. THE RED OVAL INDICATES THE ATTENUATION ZONE (GAS SHADOW) CENTERED AT THE TOP OF THE CINCINNATI GROUP REFLECTOR.....	31
FIGURE 17. A 30 HZ COMMON FREQUENCY SECTION OF LINE1. THE RED OVAL INDICATES THE ATTENUATION ZONE (GAS SHADOW) CENTERED AT THE TOP OF THE CINCINNATI GROUP REFLECTOR.....	32

FIGURE 18. GAS SHADOW ON LINE 1. THE PACKER SHELL AND TOP OF THE CINCINNATI GROUP ARE MARKED. THE RED BOX SHOWS THE ATTENUATION AREA AT THE TOP OF THE CINCINNATI GROUP REFLECTOR. ABOVE THE RED BOX IS AN ANOMALOUS POSITIVE REFLECTOR MARKED WITH A BLUE OVAL.....	34
FIGURE 19. INSTANTANEOUS FREQUENCIES AT THE MAXIMUM PHASE OF THE REFLECTOR CORRESPONDING TO THE TOP OF THE CINCINNATI GROUP OF LINE 1 ASSOCIATED WITH FIGURE 18 .....	35
FIGURE 20. A 10 HZ COMMON FREQUENCY SECTION OF LINE3. THE RED BOX INDICATES CDP 1143 TO CDP 1161 AS THE ATTENUATION ZONE (GAS SHADOW) CENTERED AT THE TOP OF THE CINCINNATI GROUP .....	36
FIGURE 21. A 20 HZ COMMON FREQUENCY SECTION OF LINE3. THE RED BOX INDICATES CDP 1143 TO CDP 1161 AS THE ATTENUATION ZONE (GAS SHADOW) CENTERED AT THE TOP OF THE CINCINNATI GROUP .....	37
FIGURE 22. A 30 HZ COMMON FREQUENCY SECTION OF LINE3. THE RED BOX WAS MARKED FROM CDP 1143 TO CDP 1161 AS THE ATTENUATION ZONE (GAS SHADOW) CENTERED THE TOP OF THE CINCINNATI GROUP .....	38
FIGURE 23. GAS SHADOW ON LINE 3. THE PACKER SHELL AND TOP OF THE CINCINNATI GROUP ARE MARKED AT 460 MS AND 510 MS RESPECTIVELY. THE RED BOX INDICATES ATTENUATION AREA AT THE TOP OF THE CINCINNATI GROUP. AN ANOMALOUS POSITIVE REFLECTOR RIGHT IS MARKED WITH A BLUE OVAL .....	39
FIGURE 24. INSTANTANEOUS FREQUENCIES AT THE MAXIMUM PHASE OF THE REFLECTOR CORRESPONDING TO THE TOP OF THE CINCINNATI GROUP IN LINE 3 ASSOCIATED WITH FIGURE 23 .....	40

FIGURE 25. A 10 HZ COMMON FREQUENCY SECTION OF LINE 5. THE RED BOX INDICATES	
CDP 2245 TO CDP 2265 THE ATTENUATION ZONE (GAS SHADOW). ....	42
FIGURE 26. A 20 HZ COMMON FREQUENCY SECTION OF LINE 5. THE RED BOX INDICATES	
CDP 2245 TO CDP 2265 AS THE ATTENUATION ZONE (GAS SHADOW). ....	43
FIGURE 27. A 30 HZ COMMON FREQUENCY SECTION OF LINE 5. THE RED BOX INDICATES	
CDP 2245 TO CDP 2265 AS THE ATTENUATION ZONE (GAS SHADOW). ....	44
FIGURE 28. GAS SHADOW IN LINE 5. THE PACKER SHELL AND TOP OF THE CINCINNATI	
GROUP ARE MARKED. THE RED BOX IS ATTENUATION AREA IN THE TOP OF THE	
CINCINNATI GROUP. AN ANOMALOUS POSITIVE REFLECTOR IS MARKED WITH A BLUE	
OVAL. ....	45
FIGURE 29. INSTANTANEOUS FREQUENCIES AT THE MAXIMUM PHASE OF THE REFLECTOR	
CORRESPONDING TO THE TOP OF THE CINCINNATI GROUP OF LINE 5 ASSOCIATED WITH	
FIGURE 28. ....	46
FIGURE 30. A 10 HZ COMMON FREQUENCY SECTION OF LINE 6. THE RED TRAPEZOID	
INDICATES CDP 2771 AND CDP2790 AS THE ATTENUATION ZONE (GAS SHADOW).....	47
FIGURE 31. A 20 HZ COMMON FREQUENCY SECTION OF LINE 6. THE RED TRAPEZOID	
INDICATES CDP 2771 TO CDP 2782 AS THE ATTENUATION ZONE (GAS SHADOW).....	48
FIGURE 32. A 30 HZ COMMON FREQUENCY SECTION OF LINE 6. THE RED TRAPEZOID	
INDICATES CDP 2272 TO CDP 2280 AS THE ATTENUATION ZONE (GAS SHADOW).....	49
FIGURE 33. GAS SHADOW IN LINE 6. THE PACKER SHELL AND TOP OF THE CINCINNATI	
GROUP ARE MARKED. THE RED TRAPEZOID INDICATES ATTENUATION AREA AT THE TOP	
OF THE CINCINNATI GROUP REFLECTOR. ....	50

FIGURE 34. INSTANTANEOUS FREQUENCIES AT THE MAXIMUM PHASE OF THE REFLECTOR CORRESPONDING TO THE TOP OF THE CINCINNATI GROUP OF LINE 5 ASSOCIATED WITH FIGURE 33. ....	51
FIGURE 35. HIGH INITIAL GAS PRODUCTION ZONE IN INITIAL PRODUCTION MAP WITH GAS SHADOWS MARKED WITH RED OVALS.. ....	53

## **Acknowledgement**

I would like to express my deep gratitude to my advisor Dr. Doyle Watts for his support and guidance during my thesis writing. Without his help, I could not go that far.

I would like to thank my committee members: Dr. David Dominic and Dr. Ernest Hauser for their advice throughout my thesis work.

I also would like to extend my gratitude to the EES Department for the financial support when I was a graduate student; to the Ohio Geological Survey for the well log data; and to the seismic data donator NGO; to CGG for providing Hampson Russell Software package. Funding for Neuralog licensing was provided through a donation by Erika and Jeffrey Reimer.



# **1 Introduction**

## **1.1 Gas Shadow**

In the 1960s, the development of digital technology led to the discovery of direct indicators of natural gas reservoirs known as bright spots. These zones of very bright reflections on seismic reflection records may be caused by the presence of natural gas reservoirs within water-saturated zones.

In addition to bright spots, low frequency shadows are also regarded as direct indicators of natural gas. Taner et al. (1979) first noted that the frequency content of reflectors immediately beneath natural gas and condensate reservoirs contained enhanced lower apparent frequencies. These shadows are attributed to high attenuation of seismic waves transmitted through gas reservoirs, reducing the amplitudes and frequency content of reflectors beneath a gas reservoir but also enhancing low frequencies. However, there is still no known mechanism or theory that predicts the observed shift of spectral energy from high to low frequencies (Castagna et al., 2003). Ebrom (1996) proposed a number of alternative explanations for gas shadows that have nothing to do with the presence of hydrocarbons. Besides intrinsic attenuation, these gas shadows might be caused by stacking or data processing issues such as wave trains associated with deconvolution. Despite these uncertainties, commercial processing houses promote the identification of shows as a viable exploration tool.

Low frequency gas shadows are different from the gas shadows identified in Ohio. Low frequency shadows are accessible broadly. Not only can it describe the high attenuations associated with hydrocarbons, but also the attenuations in water-saturation zones or in

unconsolidated Quaternary formations. Furthermore, low frequency shadows occur when low frequencies are enhancement and high frequencies are reduced under time-frequency analysis (Castagna et al., 2003). The concept of gas shadows is more straightforward, because it only refers to simple attenuation of the signal at all frequencies beneath gas reservoirs. Bey (2011) and Haneberg-Diggs (2014) reported gas shadows within a gas storage field in Ohio. Unlike enhancement at lower frequencies, a gas shadow attenuates all frequencies in otherwise continuous reflectors. Moreover, the gas shadow displays a dramatically low frequency zone in the average frequency plot. In this thesis, I quantify how lateral continuous seismic reflectors lose their coherency in gas shadows using a time-frequency analysis method.

## **1.2 Time-Frequency Analysis**

The Fourier Transform is a powerful method that decomposes a signal into different frequencies with different amplitudes to create a spectrum of the signal. After application of the Fourier Transform, the display in the frequency domain allows a different perspective and allows processing steps such as band pass filtering. However, the Fourier Transform cannot reveal the instantaneous attributes of the signal or time variations in frequency content. To apply the Fourier Transforms to a time series, one needs to create a window function and assumes that the signal is stationary in that window. The length of the window influences the results of the Fourier Transform. A short window length results in the loss of resolution in the frequency domain. Application of a long window increases the frequency resolution, but decreases the resolution in time (Castagna et

al.,2003).There is a direct tradeoff between time localization and frequency resolution (Wuet.al., 2009).

Real seismic reflection data are not stationary. The frequency content of seismic data changes with time. Obviously, the applications of the Fourier Transform to seismic data sets are therefore limited. A large number of methods are now available to accomplish time-frequency analysis, each of which has advantages and disadvantages (Marfurt, 2005; Castagna et al., 2003). For example, the continuous wavelet transform provides results in a time-scale domain rather than time-frequency domain (Wu et al., 2009). Maximum entropy can archive high frequency resolution only if the rather strict conditions of the method are not violated and should be used by those who are very experienced in the application of the method. It may produce some artificial anomalies “at given time over a wide frequency band or at a given frequency over a long time interval” (Castagna et al., 2003).

To get better resolution in both time and frequency, instantaneous spectral analysis (ISA) is an ideal method. ISA provides the continuous analysis in time and frequency domain. Time-frequency distributions were introduced to display information contained in non-stationary signals. The spectral density functions of non-stationary signals with frequency content that vary with time are of major importance in engineering.

Considering that different signals may contain the same spectral density, analysts created methods to display instantaneous frequency. Just like spectral density, the instantaneous power of a signal represents the distribution of signal energy in the time domain when coupled with instantaneous frequency (Boashash and Whitehouse, 1987).

The Wigner-Ville distribution is considered an effective tool for tracking spectral changes with time in real signals, especially in the context of instantaneous spectral analysis (Boashash and Whitehouse, 1987). Ville (1948) introduced instantaneous frequency and defined it mathematically using the concept of an analytic signal. He combined the idea of the analytic signal with the Wigner distribution that was created to study quantum mechanics. Since then, the Wigner-Ville distribution is used to study signals in the time-frequency domain. However, this method has the shortcoming of cross terms interference. This effect is encountered with a signal that has two or more separated frequencies components, producing artifacts that exhibit frequency content between the two separate frequencies (Qian et al., 1996; Roshan-Gias et al., 2007). The Smoothed Pseudo Wigner-Ville distribution is an updated version of Wigner-Ville distribution designed to eliminate this cross term interference (Flandrin, 1999). The Smoothed Pseudo Wigner-Ville uses two different smoothing windows respectively in the time domain and in the frequency domain on the Wigner-Ville distribution. The Smoothed Pseudo Wigner-Ville Distribution (SPWVD) helps the interpreter to locate the reflection events at both the time and frequency domain with higher resolution. This method is used to locate gas shadows in the Clinton interval in the Muskingum, Ohio.

### **1.3 Hydrocarbon Production History in the Clinton interval in Ohio**

Oil and gas production began in the Ohio State more than 150 years ago in Mecca Township of Trumbull County. No less than 220,000 productive oil and gas wells have been drilled in the state and approximately 60,000 of them are presently producing hydrocarbon (Oil and Gas Fields Map of Ohio, Ohio Division of Geological Survey, 2014). Muskingum County, locating at central-east part of Ohio, has been drilled for oil

and gas for more than 100 years. The Clinton interval has produced oil and gas since the later 19<sup>th</sup> century when the first Clinton well was drilled in 1887. The Clinton interval has produced 8.7 trillion cubic feet of gas, providing a continuous source of revenue for the state. The Clinton interval is a primary target for production of oil and gas, because the relatively porous and permeable sands in the Clinton interval are generally widespread. The Clinton interval is known in eastern Ohio as Silurian fluvial-deltaic deposits consisting of interbedded sandstone and shale between 50 to 120 feet in thickness (Figure 1). My study areas are both located within oil and gas production zones (Figure 1) than now include a gas storage field.

#### **1.4 Objective.**

Haneberg-Diggs (2014) analyzed seismic reflection data acquired over the Dominion East Ohio gas storage field near Canton, Ohio in the Clinton interval, applying seismic attribute analysis. He identified gas shadows associated with the Clinton interval beneath fully charged reservoirs in parts identified as having good reservoir quality on the basis of initial production of the wells before they were converted to a storage field. I continued this research by characterizing the most prominent gas shadow using time-frequency analysis. In this thesis, the Smoothed Pseudo Wigner-Ville Distribution method was employed to analyze the Clinton interval in seismic reflection data from the Dominion East Ohio Gas Storage field and seismic reflection data from Muskingum County. This method may be effective in locating subtle signatures of a natural gas reservoir. Possible gas shadows were compared to an initial production map.

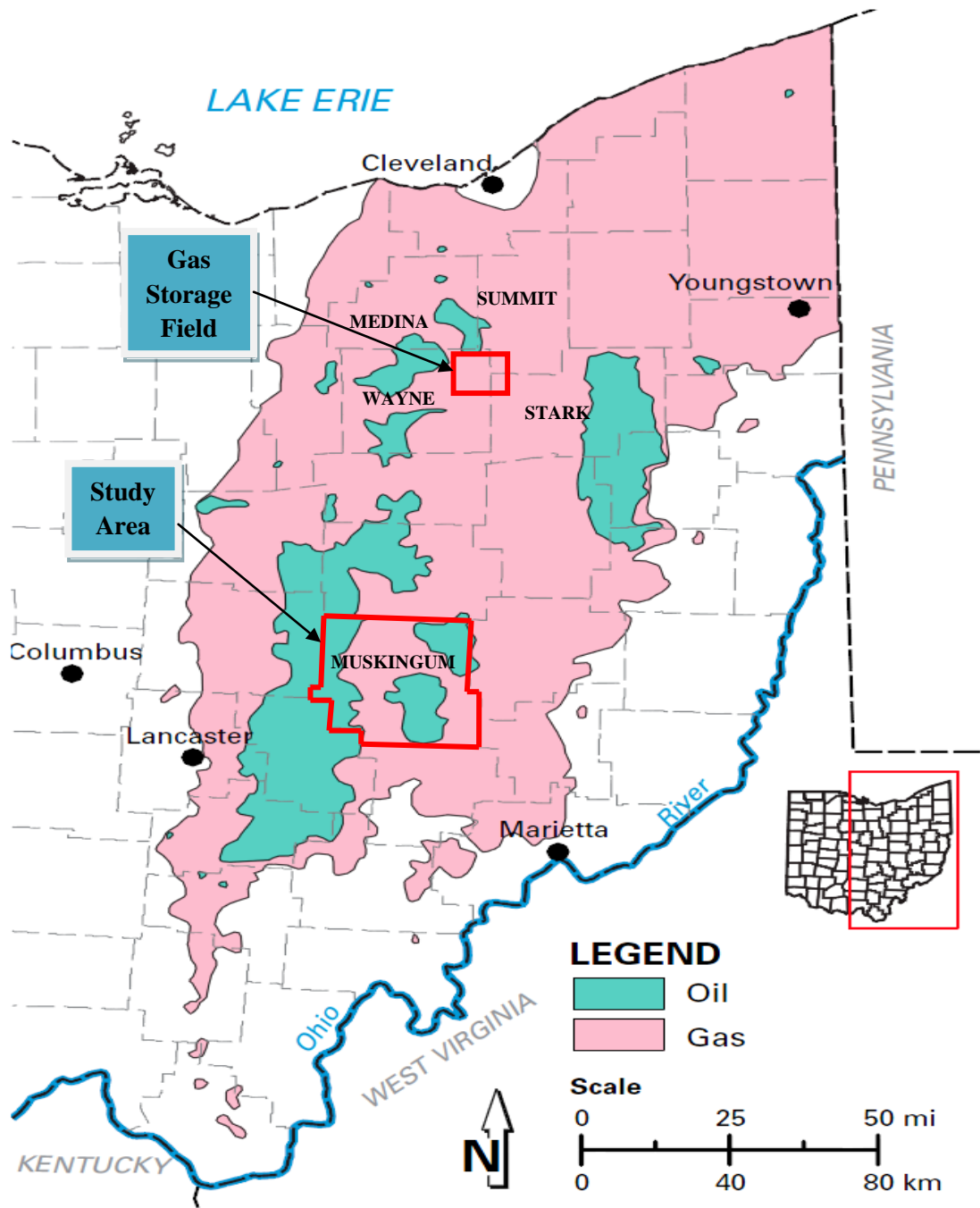


**Figure 1. Map showing location of the “the Clinton interval” oil and gas fields in Ohio (Geofacts, June 2015, Ohio Department of Natural Resources). The gas storage field and Muskingum County are marked as two red boxes.**

## **2 Geology**

### **2.1 The Clinton Interval**

The Clinton interval is a fluvial deltaic deposit in the subsurface of eastern Ohio consisting generally of three sandstone layers interbedded with shale, and siltstone. The Clinton interval was deposited during the early Silurian and unconformably overlies the Ordovician Queenstone Shale (Haneberg-Diggs, 2014). Above the Clinton interval is the Dayton Limestone Formation, known to drillers as the Packer Shell limestone. While the Clinton interval is not a reflector in seismic data, the Packer Shell reflector is generally the strongest and most continuous reflector on seismic profiles gathered in eastern Ohio. Generally, the Clinton interval is divided by drillers into three sandstone layers. From bottom to top, white Clinton, red Clinton and stray Clinton (Figure 2).

### **2.2 Previous Study of the Clinton interval**

Pepper et al. (1953) investigated the Clinton interval in Canton, Dover, Massillon and Navarre quadrangles covering about 880 square miles in eastern Ohio. The studies based on driller's logs and well samples concluded that the Clinton interval was subdivided into three sands deposited as distributary-channel and offshore-bar deposits. The authors concluded that stratigraphic traps contain the oil or gas deposits and that structure appears to be relatively unimportant in localizing the accumulation of the petroleum.

SYSTEM/ PERIOD	SERIES	GROUP	LITHOSTRATIGRAPHIC UNITS	
			SIGNIFICANT UNITS	DRILLERS' TERMS
<b>SILURIAN</b>	<b>WENLOCK</b>	<b>CLINTON</b>	Dayton Ls	"Packer Shell"
	<b>LLANDOVERY</b>	<b>MEDINA</b>	"Clinton" ss	"Stray Clinton" "Red Clinton" "White Clinton"  "Medina ss"
<b>ORDOVICIAN</b>	<b>UPPER</b>	<b>CINCINNATI</b>	Queenston Sh	"Red Medina"
			Utica sh	
	<b>MIDDLE</b>		Point Pleasant Fm	

Fm = Formation    Gp = Group    Sh = Shale    Ss = Sandstone    Ls = Limestone  
 ~~~~~ Unconformity

**Figure 2. Generalized lithostratigraphic units of the Clinton interval and vicinity (Geofacts, June 2015, Ohio Department of Natural Resources).**



Knight (1969) investigated the Clinton interval in northeastern Ohio. He also found that geological structure seems have no control on the distribution of hydrocarbons in the study area. Oil apparently is present generally in the White Clinton whereas natural gas is found in both the Red Clinton and White Clinton. He stated that hydrocarbon production in the Clinton interval generally is limited due to lower porosity and permeability.

Natural gas is the dominant hydrocarbon because of the chemical conditions under which the source rock, the Cabot Head Shale, was deposited. Geologically, he explained that the Clinton interval was deposited in small deltas along a fluctuating shore line in a relatively arid climate. The conditions were favorable for the limited generation and accumulation of hydrocarbon.

Keltch (1985) focused the studies on detailed depositional systems in Guernsey Country, Ohio. Making use of geophysical well logs, sandstone isopach maps and slice isopach maps, he inferred that high-constructive cratonic delta systems deposits occurred in laterally discontinuous sandstone bodies deposited as three different types: distributary mouth bars, distributary channel fills and delta plain point bars. Distributary mouth bar sandstones are characterized by coarsening upward log signatures. Distributary channel fill deposits are the most prolific reservoirs, are superimposed on underlying mouth bar deposited have blocky log signatures and form linear, narrow “shoestrings”. Point bar deposits fine upward and have ovoid to kidney shaped isopach patterns. Mikan (1973) also made a detailed study of paleoenvironment of the Clinton sandstone in Guernsey Country, Ohio. He recognized deltaic features by applying gamma ray logs.

Wilson (1988) investigated the depositional environments and structure of the Clinton interval. He concluded that high natural gas production was associated with thick, porous sands. This observation, however, as Shadrach (1989) stated in his thesis, contradicts the conclusion of Knight (1969) that purity and thickness of sands were not a significant factor in production of gas from the Clinton interval.

The Clinton interval is thought to have four major depositional phases: an initial marine transgression deposition; a regressive delta depositing prodelta shale overlain by delta front and delta plain sandstone; a depositional phase that formed sandstone and finally a marine transgression that deposited marine shale and shelf carbonates (Coleman and Prior, 1980; Visher et. al., 1971). The vertical sequence of Lower Silurian lithology is an excellent example of a cratonic delta system (Brown, 1979; Swanson, 1979; Shannon and Dahl, 1971).

### **3 Method**

#### **3.1 Time-Frequency Characterization of a known Ohio Gas Shadow**

I first analyzed the time-frequency content of a gas shadow reported from 2D seismic reflection data acquired from the Gabor Dominion East Ohio gas storage field near Canton Ohio. These 2D seismic data were collected by Wright State University using vibroseis source. The aim of this survey was to compliment a low frequency survey conducted by Spectraseis in a monitoring well to acquire velocity information in the vicinity of the reservoir. Bey (2011) and Haneberg-Diggs (2014) both analyzed aspects of these seismic data. Wytovich (2010) did reservoir analysis of the area including the construction of isopach and net sand isolith maps for the total Clinton interval using 2D seismic data and digitized logs from 348 wells. Bey (2011) and Haneberg-Diggs (2014) both described complex seismic attributes from the gas reservoir in the Clinton interval associated with gas shadows. Their results showed a clear relationship between gas reservoir and gas shadows indicating gas shadows could be a useful exploration tool.

The east-west trending seismic line from the gas storage field was selected for time-frequency analysis as it had the clearest indication of a gas shadow. The line had 353 CDPs (Common Depth Points) ranging from CDP 4003 to CDP 4355. According to Haneberg-Diggs (2014) analysis, the gas shadow beneath the Clinton interval was centered at CDP 4208 as shown in Figure 3 with clear attenuation from 510 ms to 570 ms. Several otherwise continuous seismic reflection events are interrupted by the attenuation zone. In particular, Haneberg-Diggs (2014) identified one of the reflectors as corresponding to the top of the Cincinnati Group as indicated in Figure 3.

The results of applying the SPWVD to the reflection data from the gas storage field are shown in Figure 4, Figure 5 and Figure 6. These figures show images of 10 Hz, 20 Hz and 30 Hz that all have a clear attenuation zone (represented by a red line) within which reflectors totally disappear. As found by Haneberg-Diggs (2014), the attenuation, at the top of Cincinnati Group, was centered at CDP 4208 ranging from CDP 4202 to CDP 4219. Figure 7 shows the value of instantaneous frequency at the time of the maximum phase of the reflector corresponding to the top of the Cincinnati Group. The vertical axis shows that seismic energy is reduced almost 90% at all frequencies beneath the gas shadow zone. I believed that the gas reservoir attenuated the seismic energy and created a shadow zone. While the low frequencies are at somewhat higher amplitude than higher frequencies with shadow, there is no suggestion of enhancement of low frequencies as occurs in gas shadows reported from the Gulf Mexico. SPWBD analysis quantifies the relationship between the gas shadow and attenuation. This provides an example with which exploration seismic reflection data from Muskingum County can be investigated.

### **3.2 Seismic reflection data from Muskingum County**

All the 2D seismic data were acquired in Muskingum County during the 1990's and the processed data were made available to Wright State University by NGO. There were sixteen lines in total, with thirteen lines oriented nearly north-south and the other three lines oriented approximately east-west (Figure 8). Receiver and source stations of each line were spaced 110 ft apart giving Common Depth Points (CDP) spaced nominally at 55 feet. The survey was sourced by vibroseis. Only the post-stack migrated data were

supplied for analysis. Well log data were employed using Hampson-Russell software to identify reflectors and Matlab was used to apply the instantaneous frequency analysis.

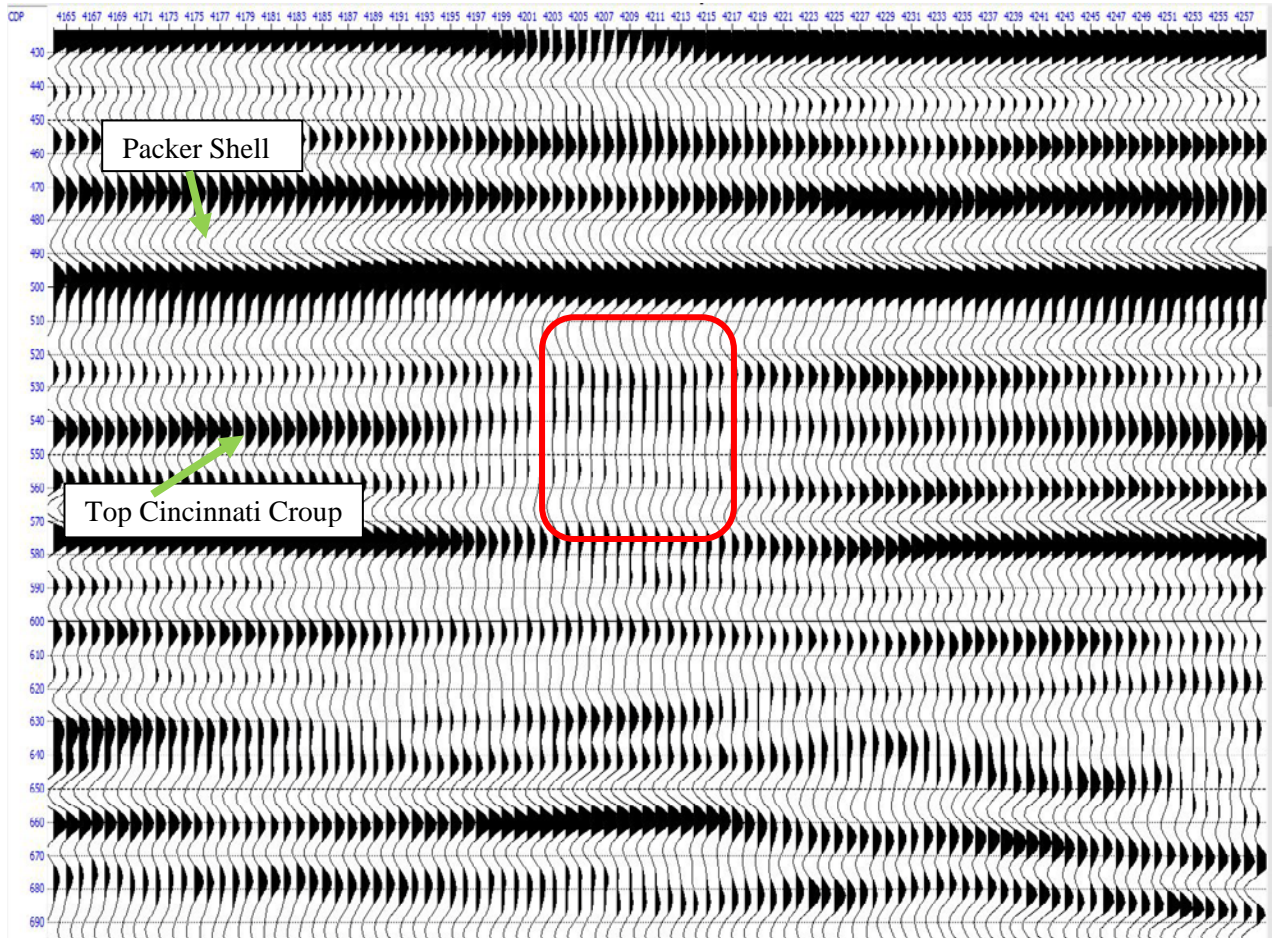


**Figure 3. Seismic line from Gabor gas storage field showing the gas shadow (after Haneberg-Diggs, 2014). The Packer Shell and Top Cincinnati Group reflectors are indicated. The red box indicates an attenuation zone due to gas shadow effect.**

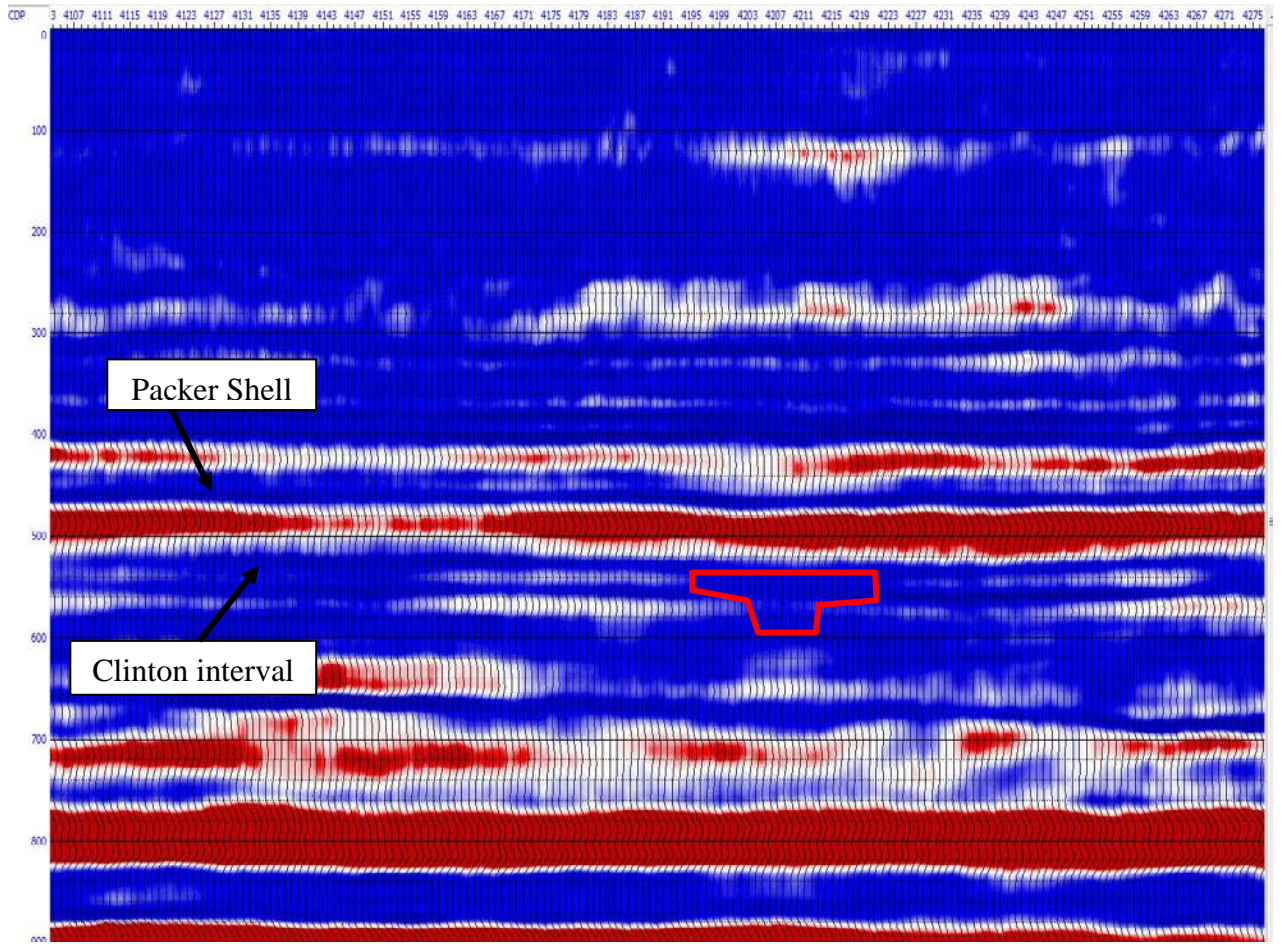


**Figure 4. A 10 Hz common frequency section. The red lines indicate the attenuation zone (gas shadow) centered at 520ms (Top of the Cincinnati Group) from CDP4202 to CDP 4219.**



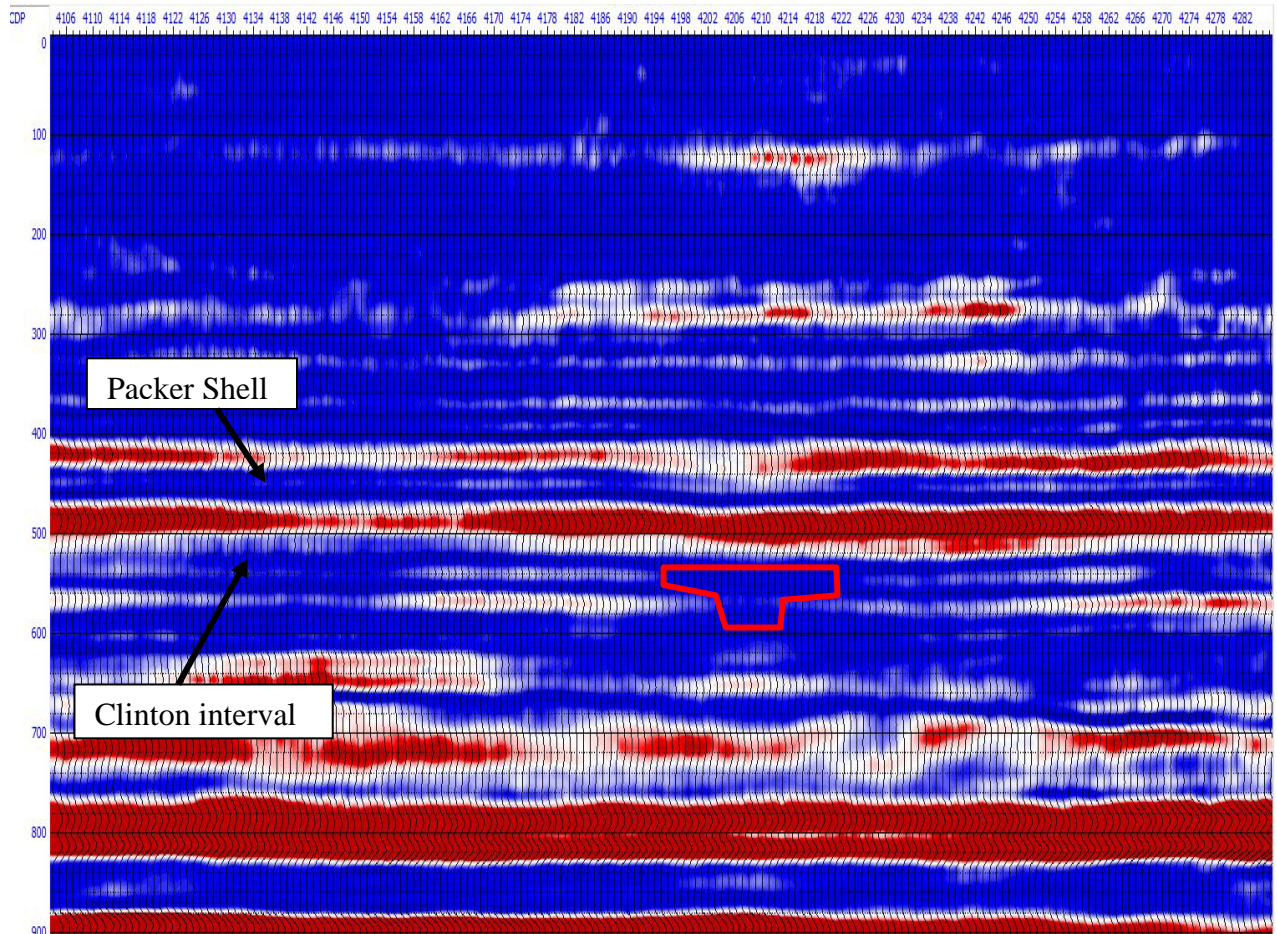


**Figure 5. A 20 Hz common frequency section. The red lines indicate the attenuation zone (gas shadow) centered at 520ms (Top of the Cincinnati Group) from CDP4202 to CDP 4219.**



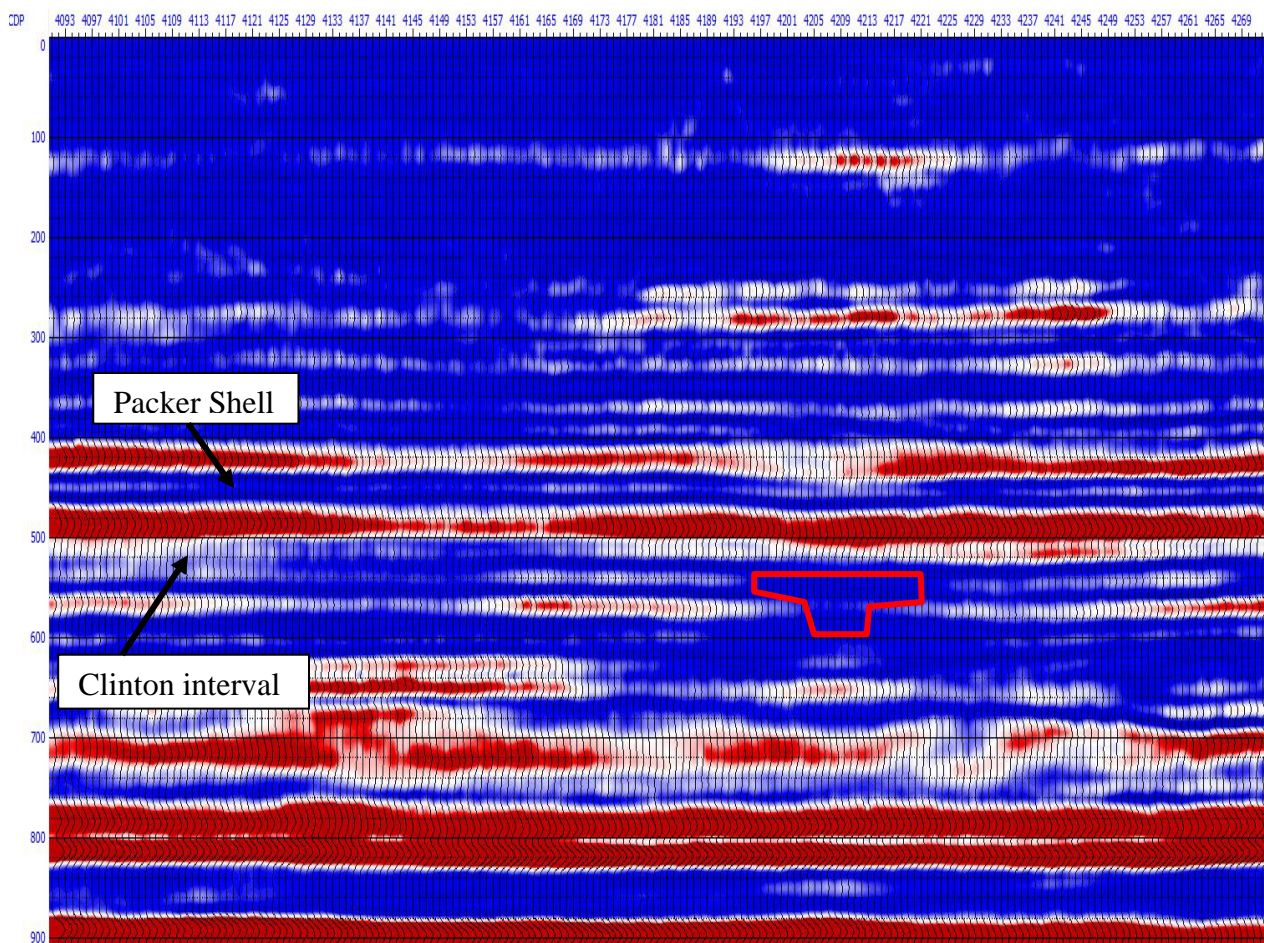


**Figure 6. A 30 Hz common frequency section. The red lines indicate the attenuation zone (gas shadow) centered at 520ms (Top of the Cincinnati Group) from CDP4202 to CDP 4212.**



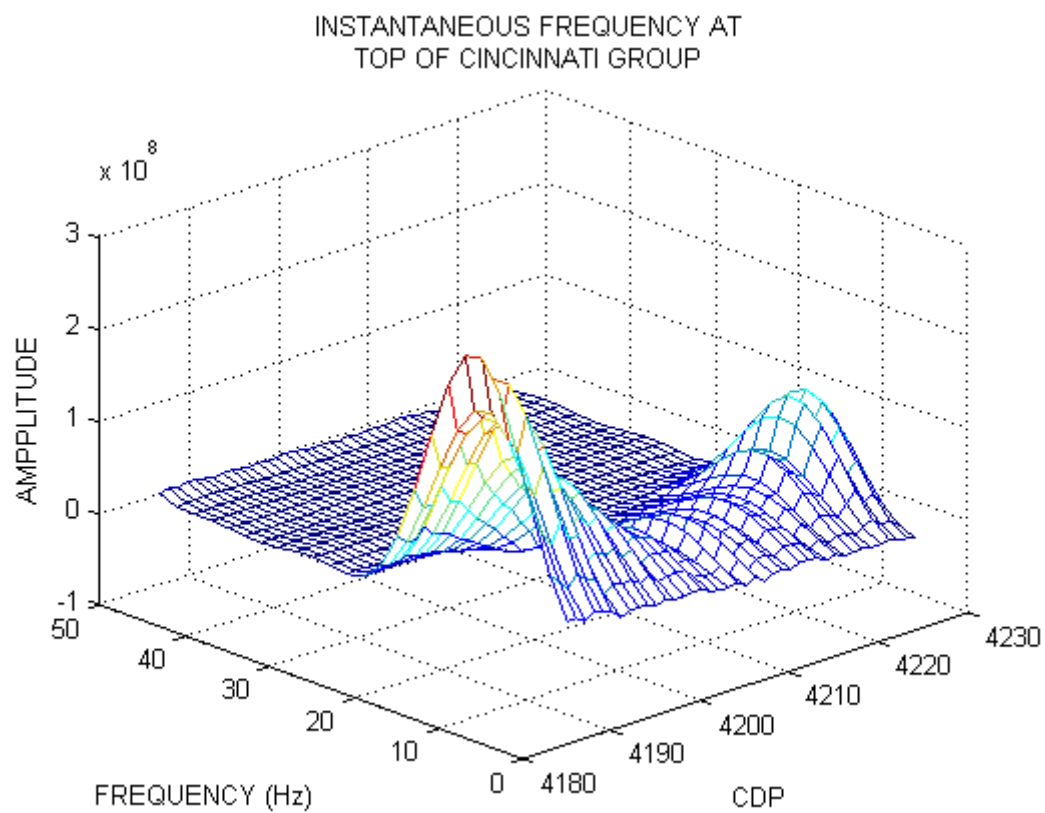


**Figure 7. Instantaneous Frequency at the maximum phase of the reflector corresponding to the top of the Cincinnati Group as indicated in Figure 3.**

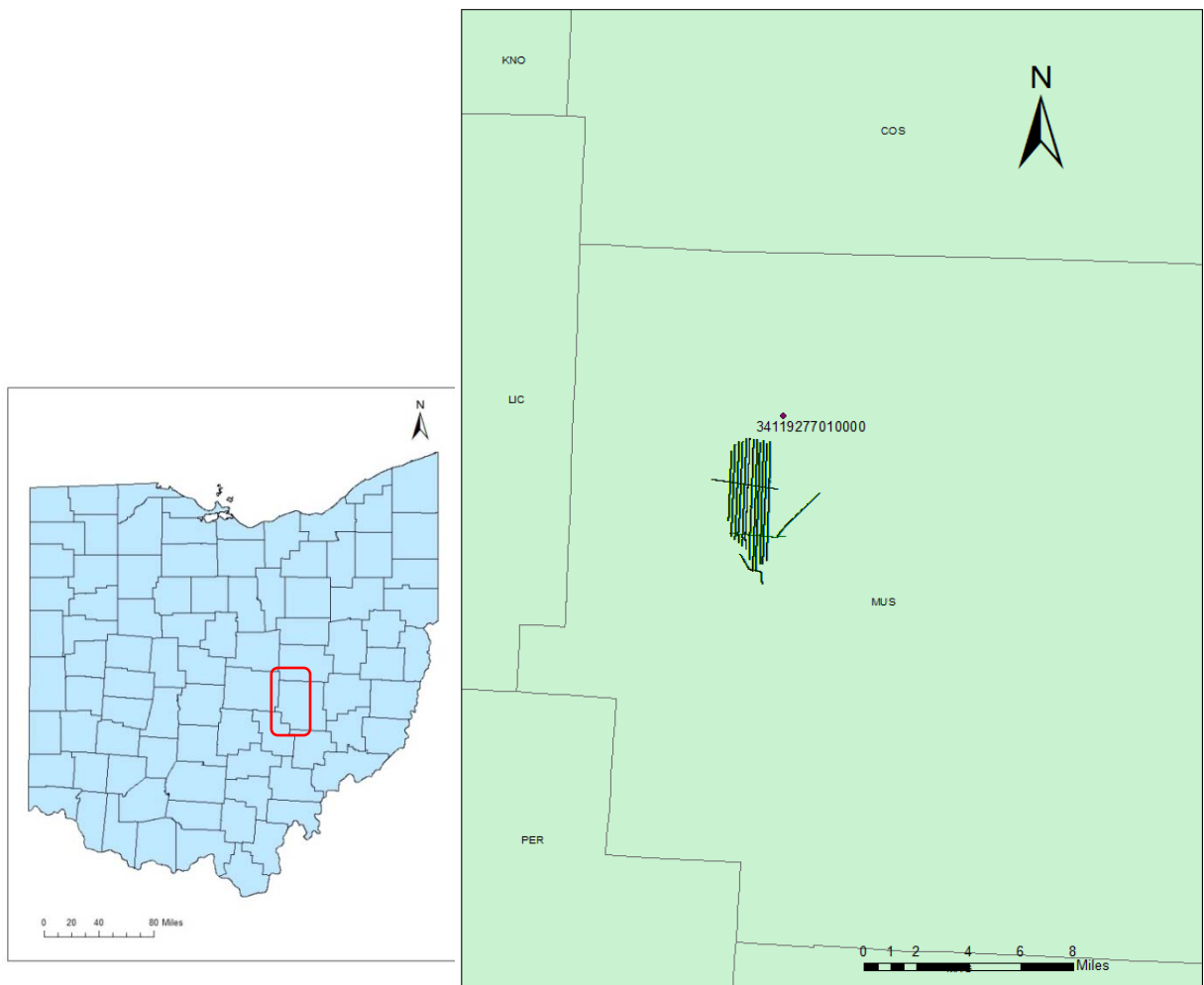


**Figure 8. Location of seismic lines in Muskingum County**

### **3.2 Identification of reflectors using Well Logs**

The well logs were supplied as .tiff files by ODNR, the Ohio Department of Natural Resources. The most useful well data are from API#34119277010000 even though it is located three miles from the nearest seismic line, because it is the only one well that contains both density and sonic logs. The well log data were digitized using the NeuraLog software package (Figure 9). The density and velocity logs are used to compute the impedance log and reflectance log used for seismic modeling.

### **3.3 Wavelet Extraction and Synthetic Traces**

The Hampson-Russell software package was used to extract a source wavelet to produce synthetic seismograms for modeling and reflector identification. The extracted wavelets that were obtained from each seismic line were correlated with the reflectivity log to produce a synthetic trace.

Since we are most interested in the Clinton interval, the two-way travel time of the wavelet extraction was centered at the Clinton interval. For the research area, the depth of Clinton interval is around 3400ft below the surface. This depth in the two-way travel time domain is 500ms about where on the seismic sections there is a strong negative reflector which is identified as the Packer Shell. Additionally, according to Haneberg-Diggs's (2014) thesis, positive side lobes on this reflector may be related to properties of the Clinton interval which may be the case in these seismic lines. When the

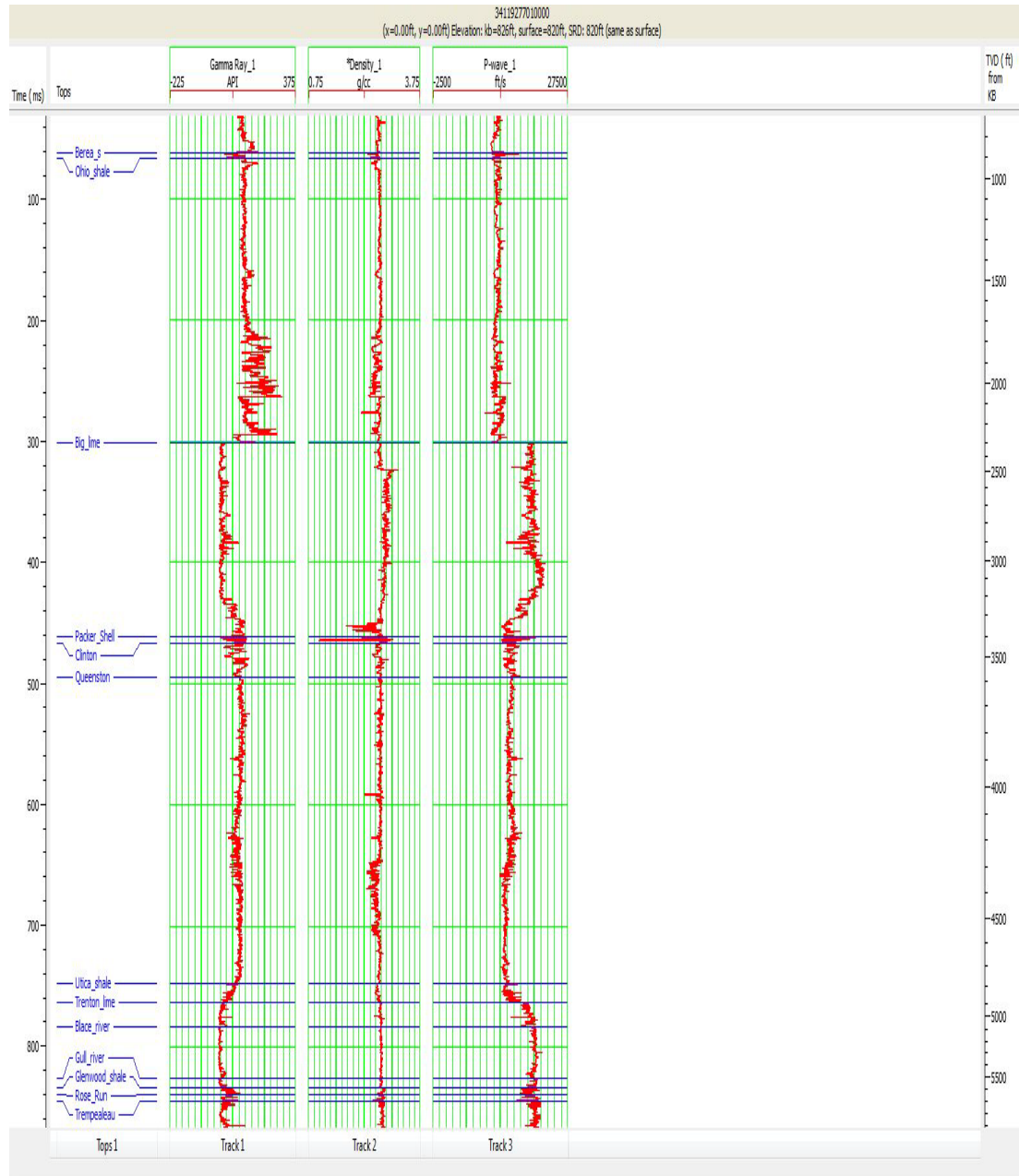


**Figure 9. Digitized well #34119277010000 density log, sonic log, gamma log with driller's tops.**

synthetic traces were tied with seismic sections the Clinton interval was also centered around 500ms. Therefore, the wavelet was extracted from the interval 300ms to 800ms on all sixteen lines (Figure 11).

Synthetic traces are a good way to estimate the how the subsurface materials respond to elastic waves. Elastic waves are reflected when the acoustic impedance changes, which means composition of geological layers alter. The synthetic seismogram representing reflectivity series along with picks of tops of formations is compared with the migrated seismic sections. Significant primary reflections should occur where there is significant contrast in acoustic impedance. Combining with driller's log, the synthetic seismogram is applied to identify the formation tops on seismograms.

A synthetic trace is generated by the following steps:

1. Collect density log data and sonic log data from a same borehole and then digitize the well data as a .las file;
2. Input the .las file, as well as formation tops into Hampson-Russell software;
3. Compute the acoustic impedance log and reflectivity logs in Hampson-Russell software (Figure 10).
4. Convolve the reflectivity log with extracted wavelet to produce a synthetic trace (Figure 11).

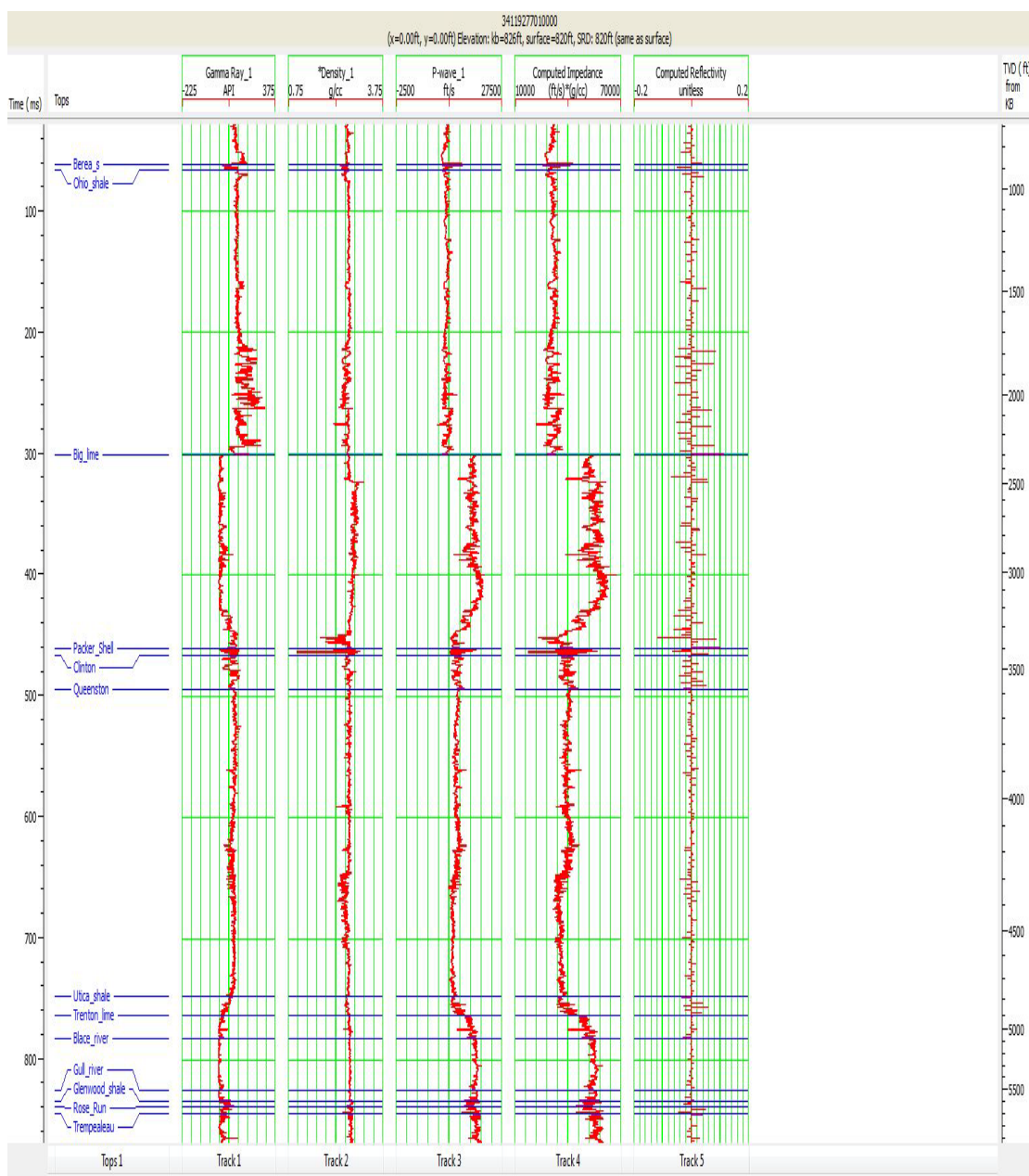


**Figure 10. The computed reflectivity log and acoustical impedance logs associated with Figure 9.**

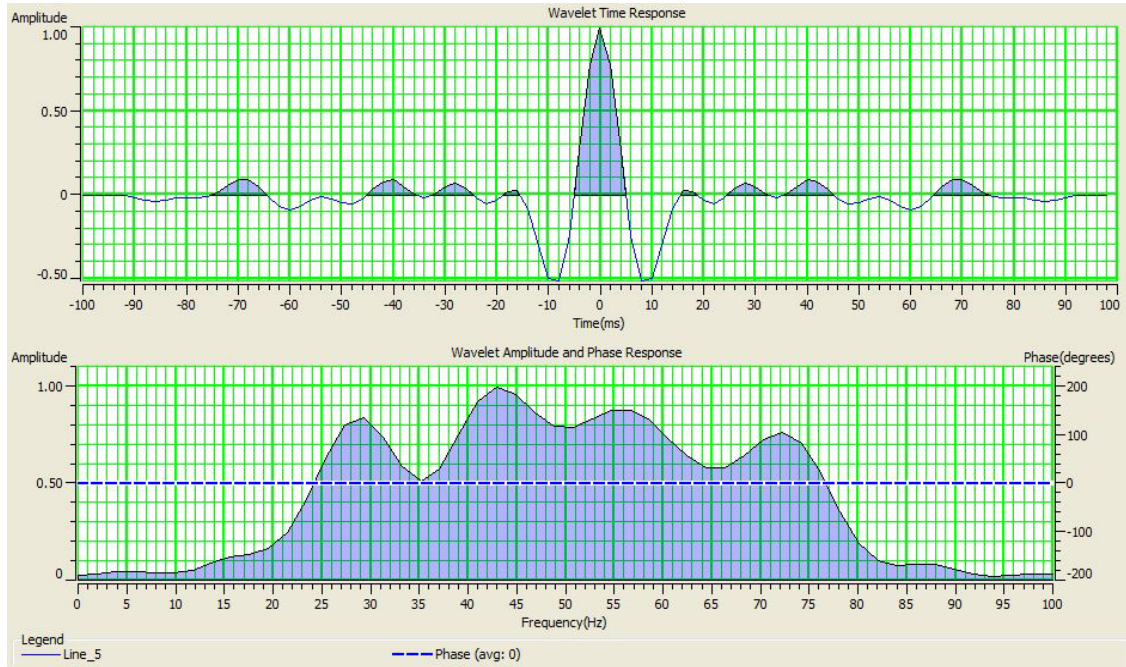


**Figure 11.Upper Figure: The extraction of the wavelet centered between 300 ms and 800 ms from line5.Lower Figure: Extracted wavelet amplitude and frequency content.**

### 3.4 Tie the synthetic trace to the seismogram

Figure 12 shows a synthetic trace calculated from the extracted wavelet and the computed reflectivity. The black traces are the synthetic seismic record while red traces are well logs or logs computed from well logs. It is clear that a very strong negative reflector is found around 460 ms. The synthetic traces may not quite match seismic traces due to the well not being located exactly on the seismic lines, but this can be easily adjusted in Hampson-Russell. After applying well log correlation with seismic lines, three prominent reflectors are picked with help of synthetic traces. The Packer Shell is picked at 480 ms

and the Clinton interval will be just beneath the Packer Shell; the Big Lime is picked at 300 ms since it is the first strong positive seismic event; the Trenton Limestone is picked around 780 ms (Figure 13) with line 5 depicted to illustrate how the processes works. All the tops in the rest of seismic lines are analyzed and picked using the same method.

### **3.5 Time-frequency Analysis**

Time-frequency analysis was conducted using Matlab scripts adapted to compute the Smooth Pseudo Wigner-Ville Distribution (SPWVD) of seismic reflection data. The seismic data are in SEG-Y format which can be read by the ReadSegy function in the Matlab package. The data are then processed into the time-frequency domain using the SPWVD. The output of the SPWVD is stored in a three dimensional array with the attributes of frequency, CDP number and time marking the cell locations. The output plots show the amplitude of a particular instantaneous frequency in the time-CDP domain.



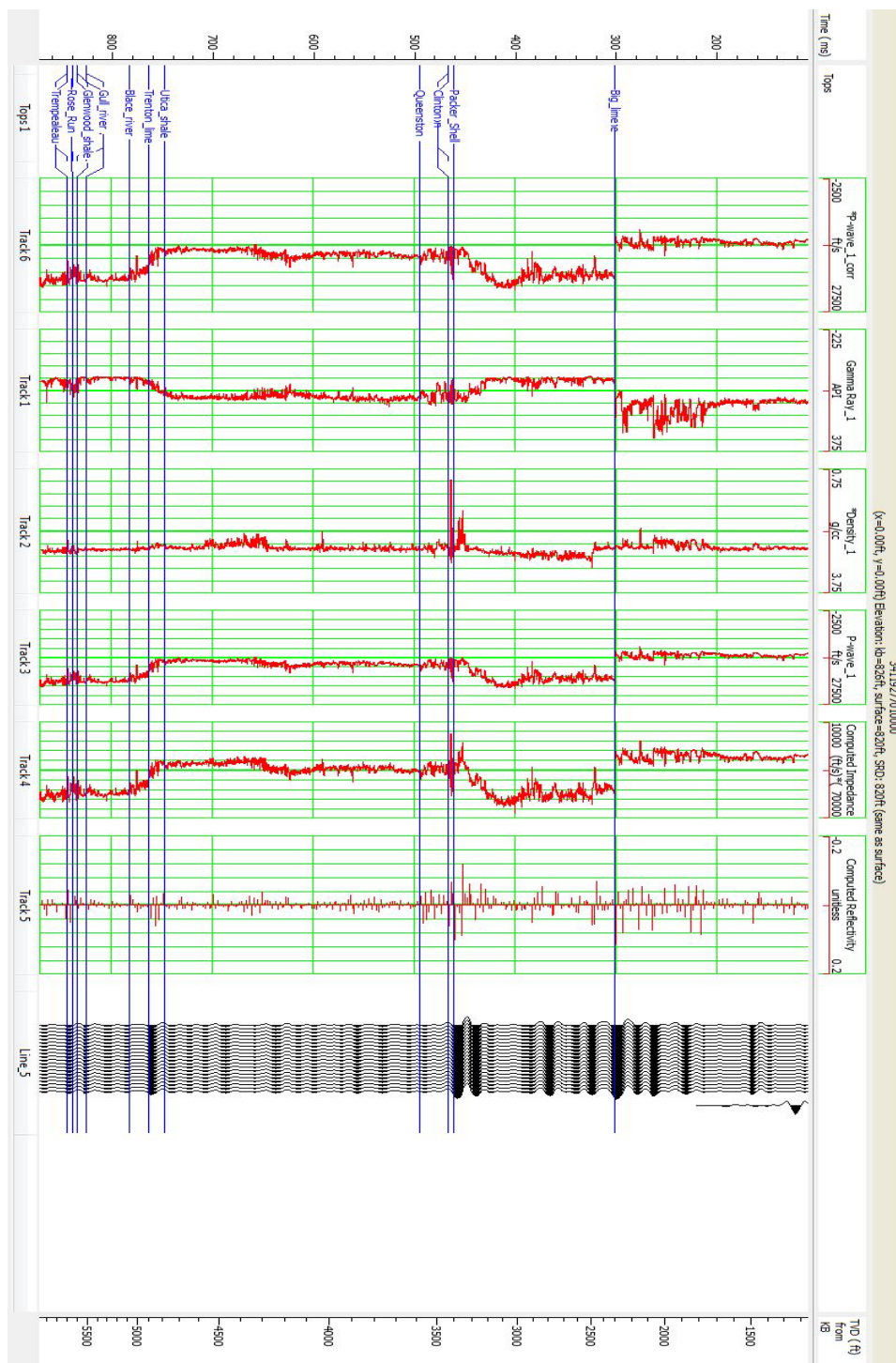


**Figure 12. The black traces are synthetic traces associated with the wavelet in Figure 11.**

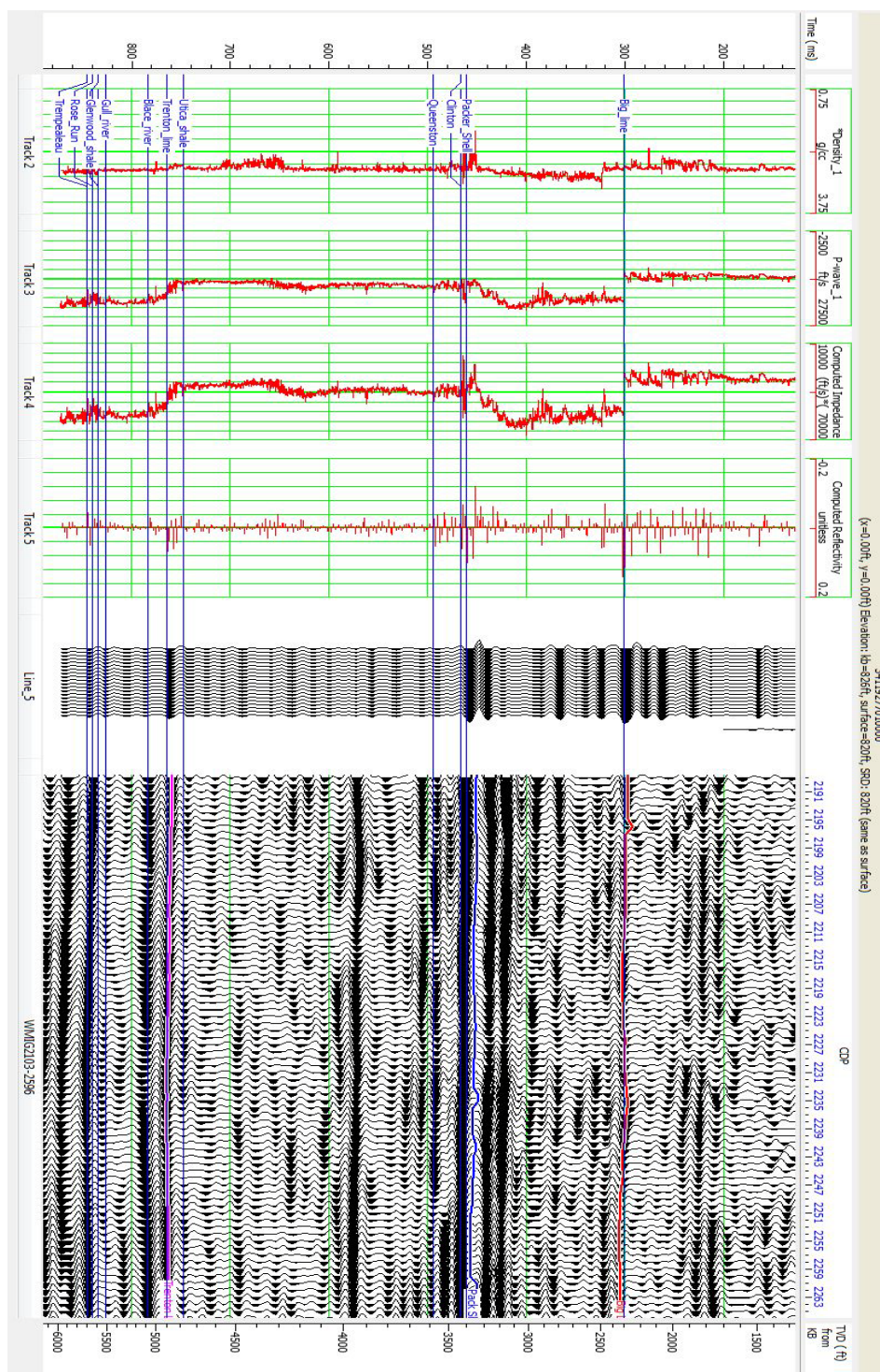


**Figure 13. Line 5 tied to synthetic traces. The Big Lime, Packer Shell and Trenton reflectors are picked.**

## **4 Results**

### **4.1 Initial Production Map**

The Initial Production (IP) map (Figure 14) was produced using ArcMAP software and data from the Ohio Department of Natural Resources. An IP map is the only indicator of the quality of gas reservoirs of the Clinton interval available since because detailed reservoir analysis is not possible using data available from the Clinton interval in Muskingum County. The problem with this approach is that known gas reservoirs are likely now depleted. Furthermore, there may be undetected and undrilled reservoirs that show gas shadows. The only way to confirm for certain is to drill a strong gas shadow but more research is recommended prior to that sort of investment. At least the IP contours provide us with a frame of reference. The contour interval on Figure 14 was set as 500 McF/day. It is clear that the several north-south lines cross over two high gas production zones as indicated by the red boxes on Figure 14. These zones were considered promising targets to look for gas shadows that might be present in associated seismic reflection data. I investigated the possibility that there might be seismic lines that exhibited the signature of the gas shadows in these zones. Although the rest of the lines, did not cross over the main gas production zone, it was still worthwhile to examine them for gas shadows.

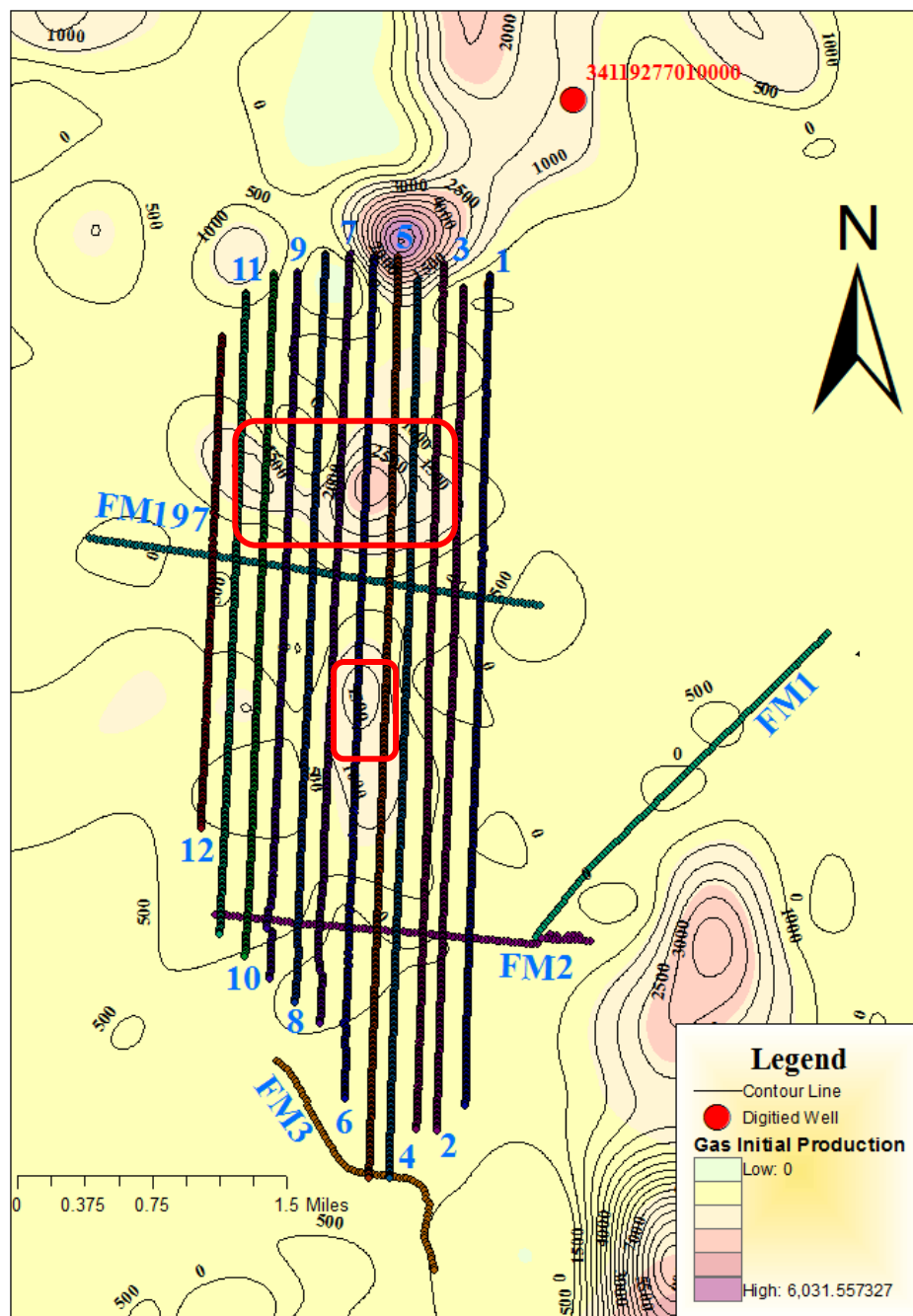


**Figure 14. Initial Production Map of Clinton gas wells in Muskingum County with seismic lines and well locations. The red boxes highlight high gas production zones.**

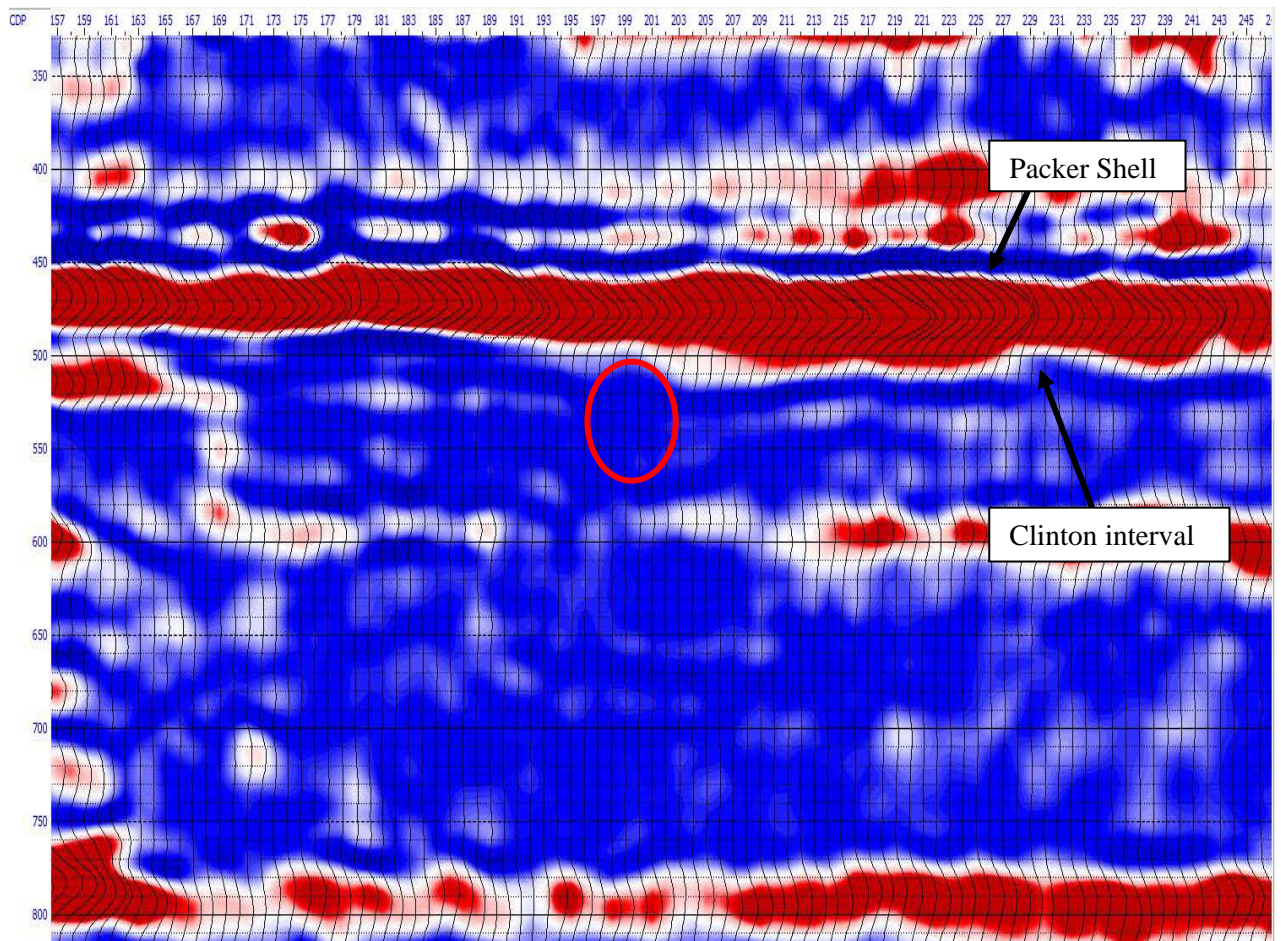
## 4.2 Results of Time-Frequency Analysis

As discussed in Chapter 3, the Packer Shell reflector was straightforward to identify on seismic sections because one eastern Ohio seismic reflection data set is invariably a strong negative, continuous reflector at about 500ms two-way travel time. The Clinton interval is located just beneath the Packer Shell reflector, but it does not produce a reflector at the resolution of seismic reflection data. However, the Clinton interval may modify the lower positive side lobe of the Packer Shell reflector (Haneberg-Diggs, 2014). The Packer Shell reflector is an indirect but effective way to locate the Clinton interval on a seismic section. I identified potential gas shadows beneath the Clinton interval on Lines 1, 3, 5 and 6. These gas shadow anomalies are revealed by applying the SPWVD at three different frequencies: 10 Hz, 20 Hz, 30 Hz as carried out previously on data from the Gabor gas storage field. The first continuous reflector immediately beneath the Clinton interval is the top of the Cincinnati Group and is traceable through the seismic sections. The top of the Cincinnati Group produces the best continuous reflector to identify gas shadows related to the Clinton interval, so I used this reflector to calculate how the gas shadows affect the frequency content employing 3D figures that plot spectral amplitude against time, CDP number and frequency.

Line 1 was the eastern most seismic line as shown in Figure 14. It has 444 CDPs from CDP 11 to CDP 455 and was 4.6 miles long. Figure 15, Figure 16 and Figure 17 show the results of the time-frequency analysis at 10 Hz, 20 Hz and 30 Hz respectively. The Packer Shell was at about 480ms and the Clinton interval located beneath it. The three figures show a clear attenuation present between CDP 195 and CDP 205, ranging from 520ms to 570ms centered at about 520ms which is the top of the Cincinnati Group

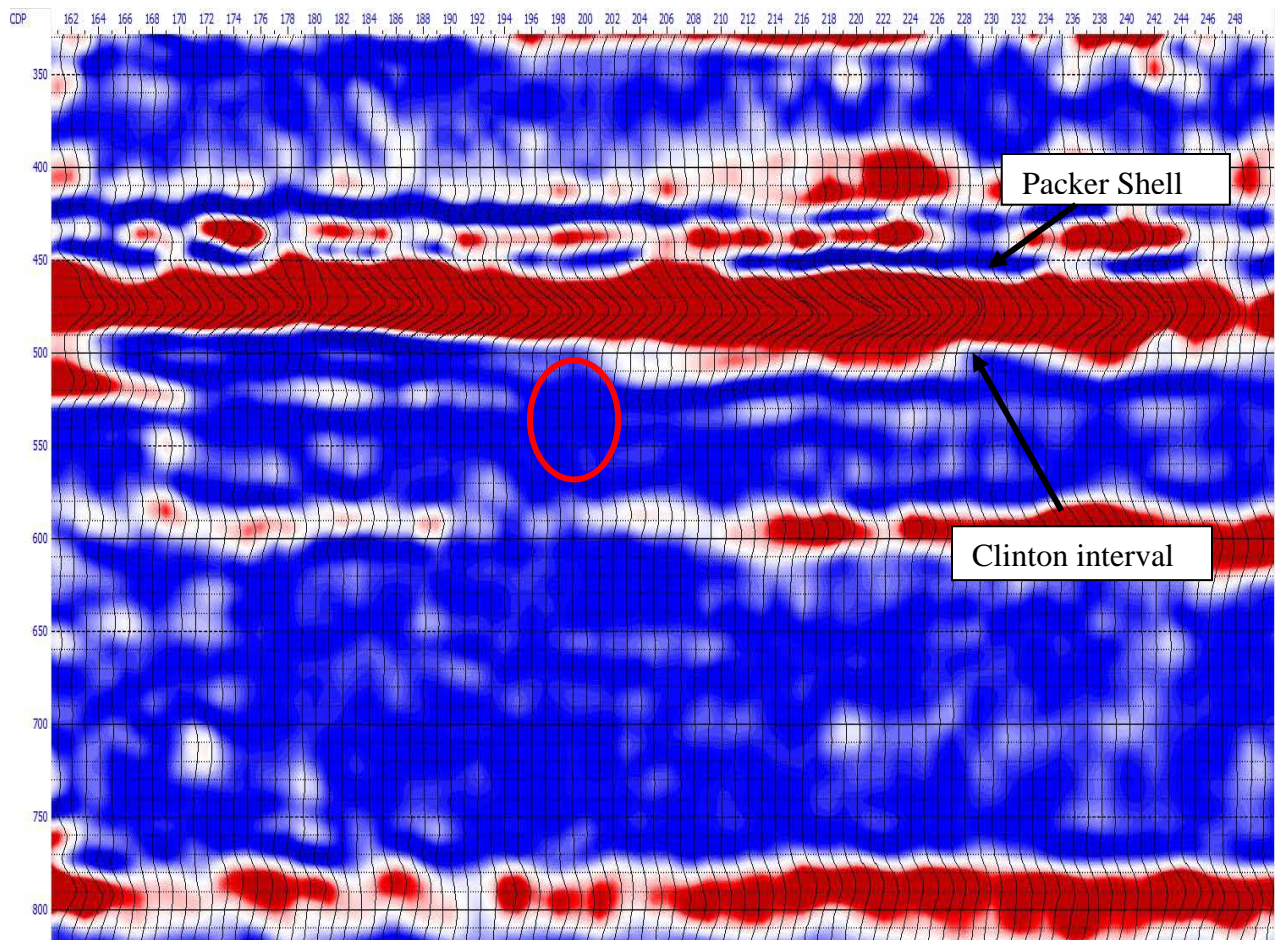


reflector. The attenuation zone was just beneath the Clinton interval and it considerably attenuated reflectors at 500ms. This attenuation even can be seen down to 600ms at 10 Hz.

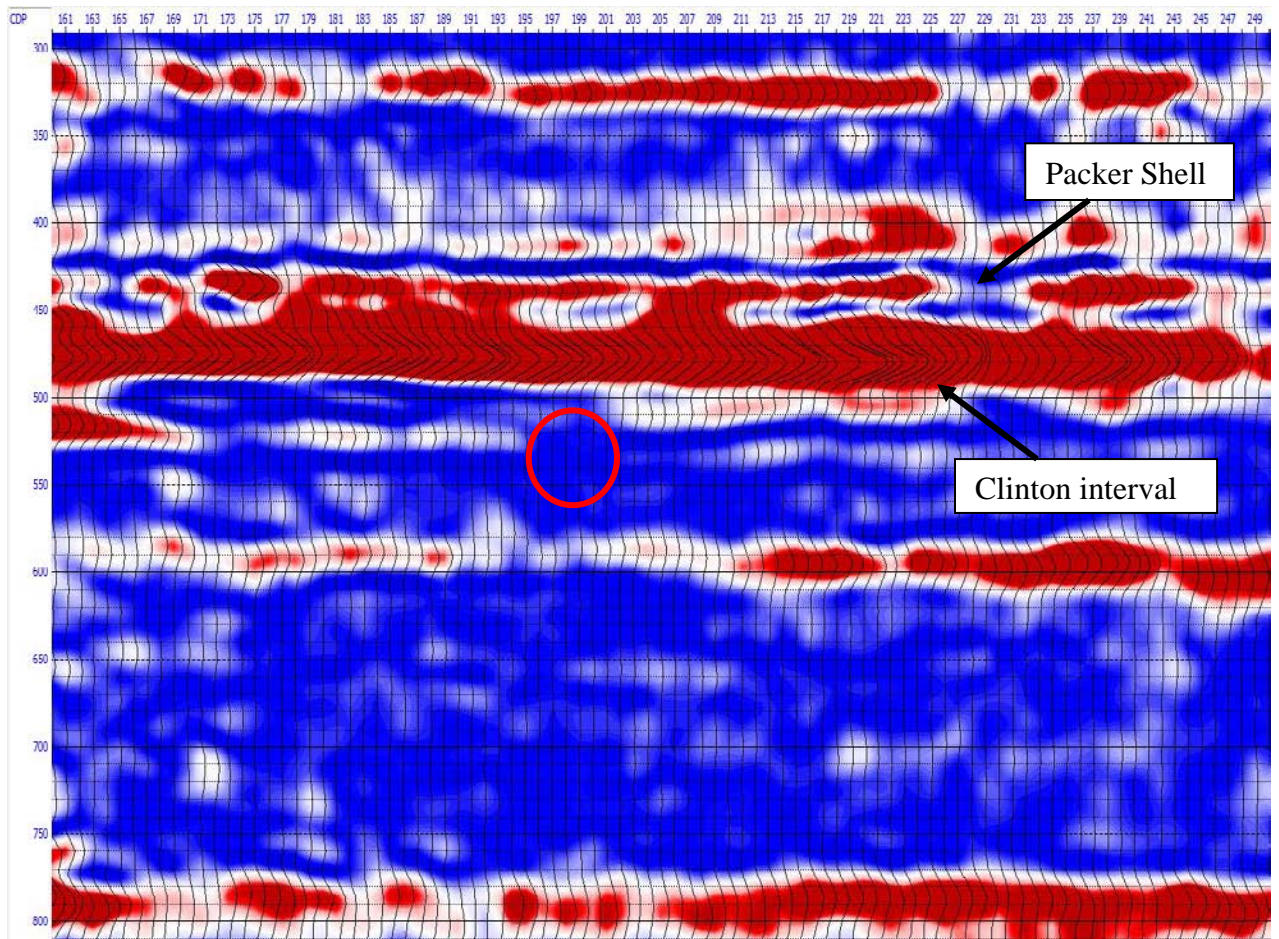


**Figure 15. A 10 Hz common frequency section of Line1. The red oval indicates the attenuation zone (gas shadow) centered at the top of the Cincinnati Group reflector.**





**Figure 16.A 20 Hz common frequency section of Line1. The red oval was marked as the attenuation zone (gas shadow) centered at the top of the Cincinnati Group reflector.**



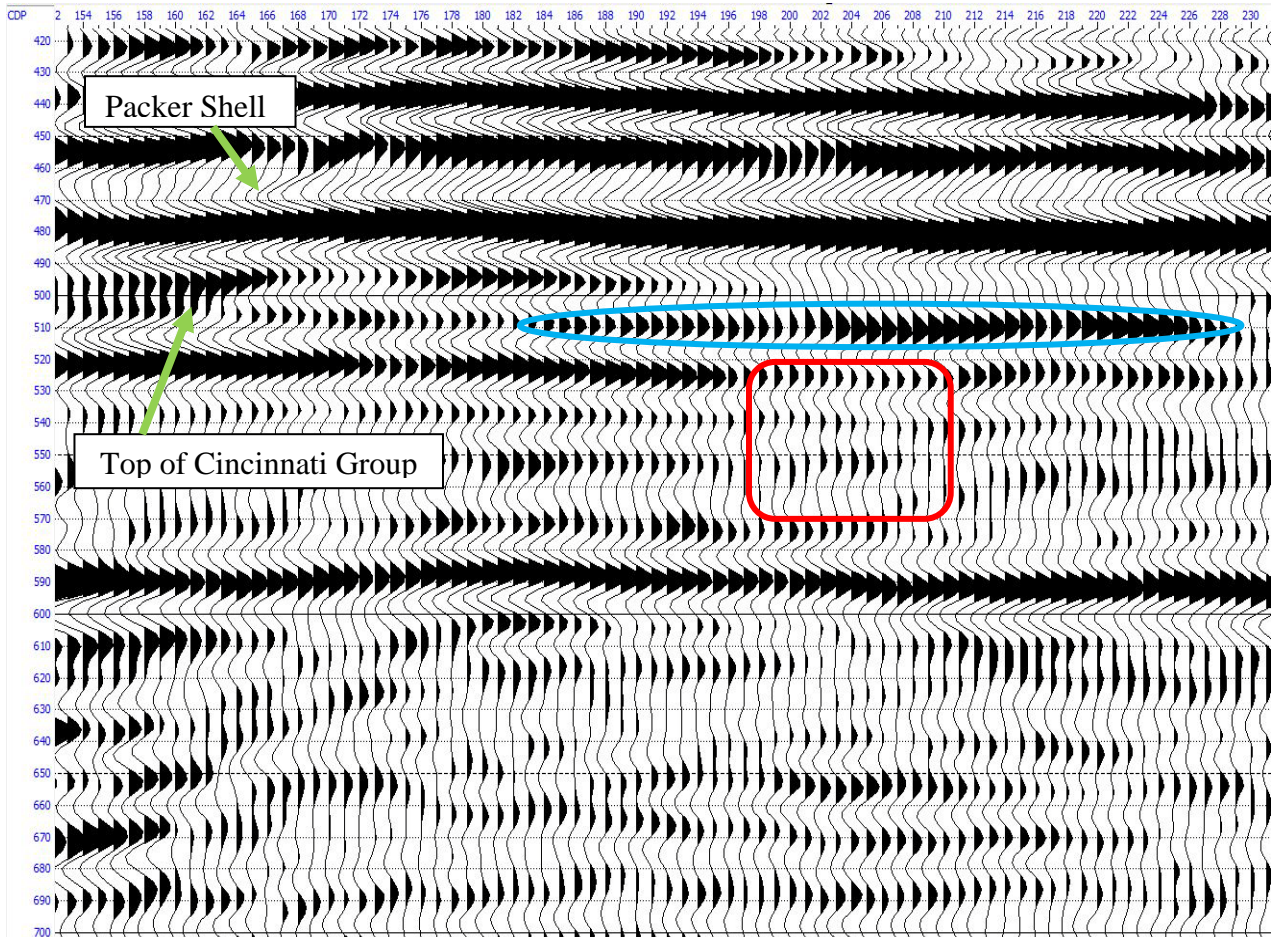
**Figure 17.** A 30 Hz common frequency section of Line1. The red oval indicates the attenuation zone (gas shadow) centered at the top of the Cincinnati Group.



Figure 18 displays the migrated Line 1 seismic section. The Packer Shell reflector is a strong negative signal at around 480ms. The first reflector below the Packer Shell is the top of the Cincinnati Group. It displays as a small positive amplitude event at about 520ms developing above the attenuated Cincinnati Group reflector. Immediately above the red box, a positive reflector is marked with a blue oval. This discontinuous reflector appears to be of low frequency content and may be associated with a change of the deposition character of the Clinton interval in which the Packer Shell side lobe develops into a full positive separate phase. Figure 19 illustrates how frequencies change within the gas shadow at the top of Cincinnati Group reflector. Within the gas shadow all frequencies are attenuated in a manner similar to that illustrated by Figure 7 which shows attenuation in data from the Gabor gas storage field. I believed that the attenuation resulted from gas reservoir, gas reservoir absorbed the seismic energy which lead to the attenuation. This is expression of the sort of gas shadow reported by Bey (2012) and Haneberg-Diggs (2014).

Line 3 had 463 CDPs ranging from CDP 1056 to CDP 1519 extending 4.8 miles in total length. Time-frequency analysis applied to Line 3 showed the most interesting results as illustrated in Figure 20, Figure 21 and Figure 22. Line 3 exhibits a clear attenuation zone between CDP 1143 and CDP 1161 centered at 500ms, from 490ms to 540ms, which is indicated by a red box on the figures. Attenuation appears just below the Clinton interval and reflectors are attenuated at all frequencies. Figure 24 shows the frequency content variation at the top of the Cincinnati Group within the shadow. Again, the behavior resembles the result from the Gabor gas storage field as illustrated in Figure 7. The Packer Shell reflector is located at about 480ms and top of the Cincinnati Group reflection event

is at about 500ms. Between the two reflectors, immediately above the gas shadow, Figure 23 shows the development of a positive reflector that correlates perfectly with the gas shadow. This may indicate the presence of a sedimentary body in the Clinton interval that favors the trapping of natural gas. Figure 24 displays how the frequency varies at the top of the Cincinnati Group with over 95% of seismic energy was absorbed in this gas shadow zone.



**Figure 18. Gas shadow on Line 1. The Packer Shell and top of the Cincinnati Group are marked. The red box shows the attenuation area at the top of the Cincinnati Group reflector. Above the red box is an anomalous positive reflector marked with a blue oval.**

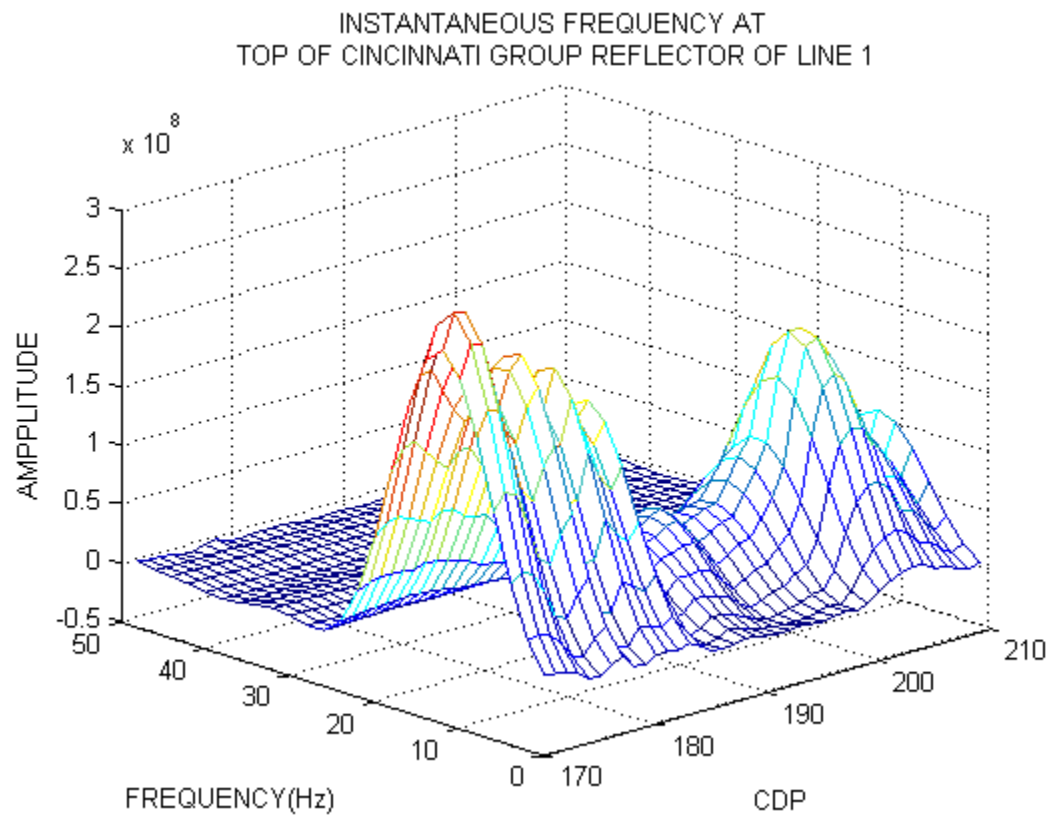


**Figure 19.**Instantaneous frequencies at the maximum phase of the reflector corresponding to the top of the Cincinnati Group in Line 1 associated with Figure 18.

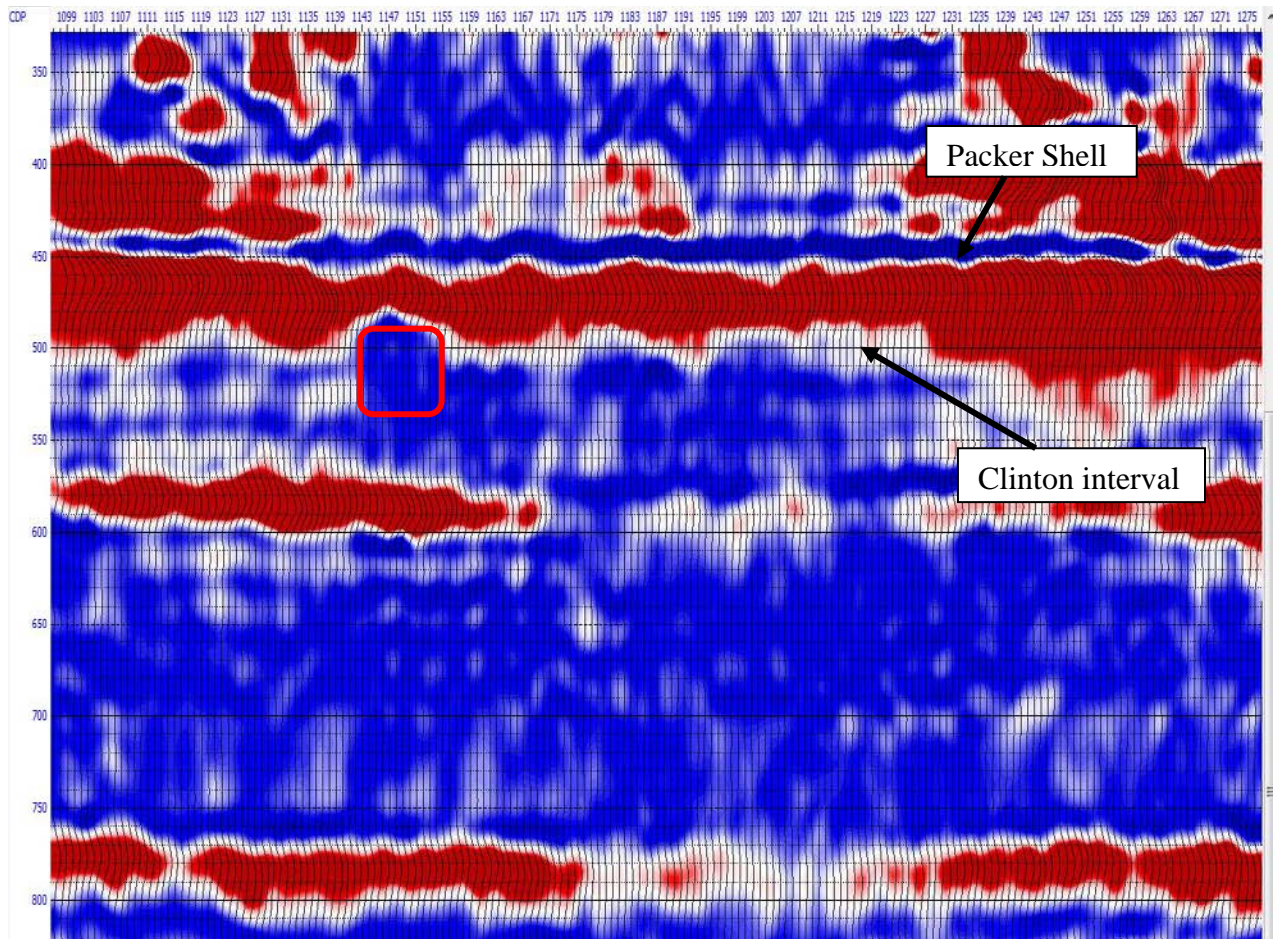


**Figure 20. A 10 Hz common frequency section of Line3. The red box indicates CDP 1143 to CDP 1161 as the attenuation zone (gas shadow) centered at the top of the Cincinnati Group.**



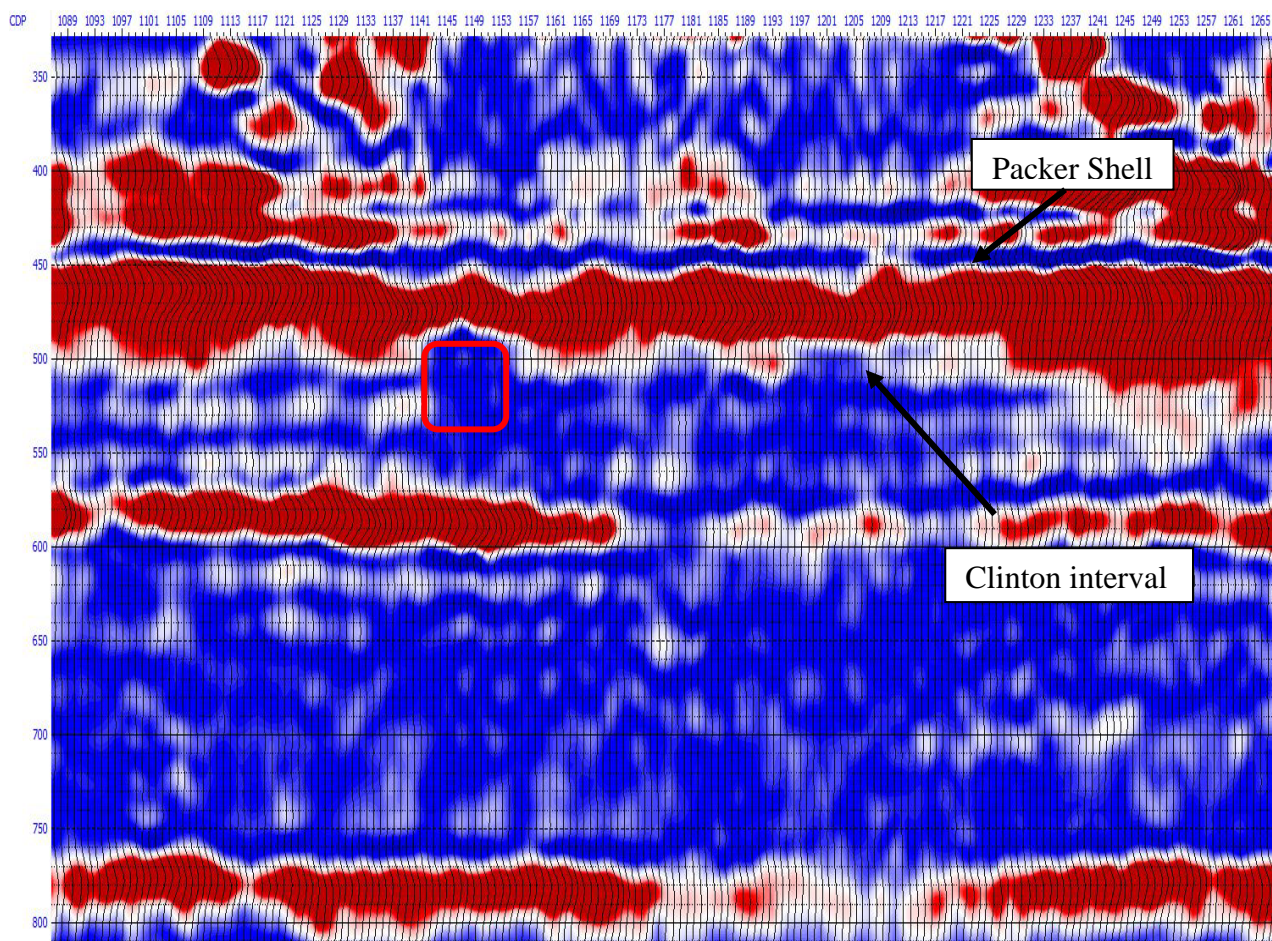


**Figure 21. A 20 Hz common frequency section of Line3. The red box indicates CDP 1143 to CDP 1161 as the attenuation zone (gas shadow) centered at the top of the Cincinnati Group.**



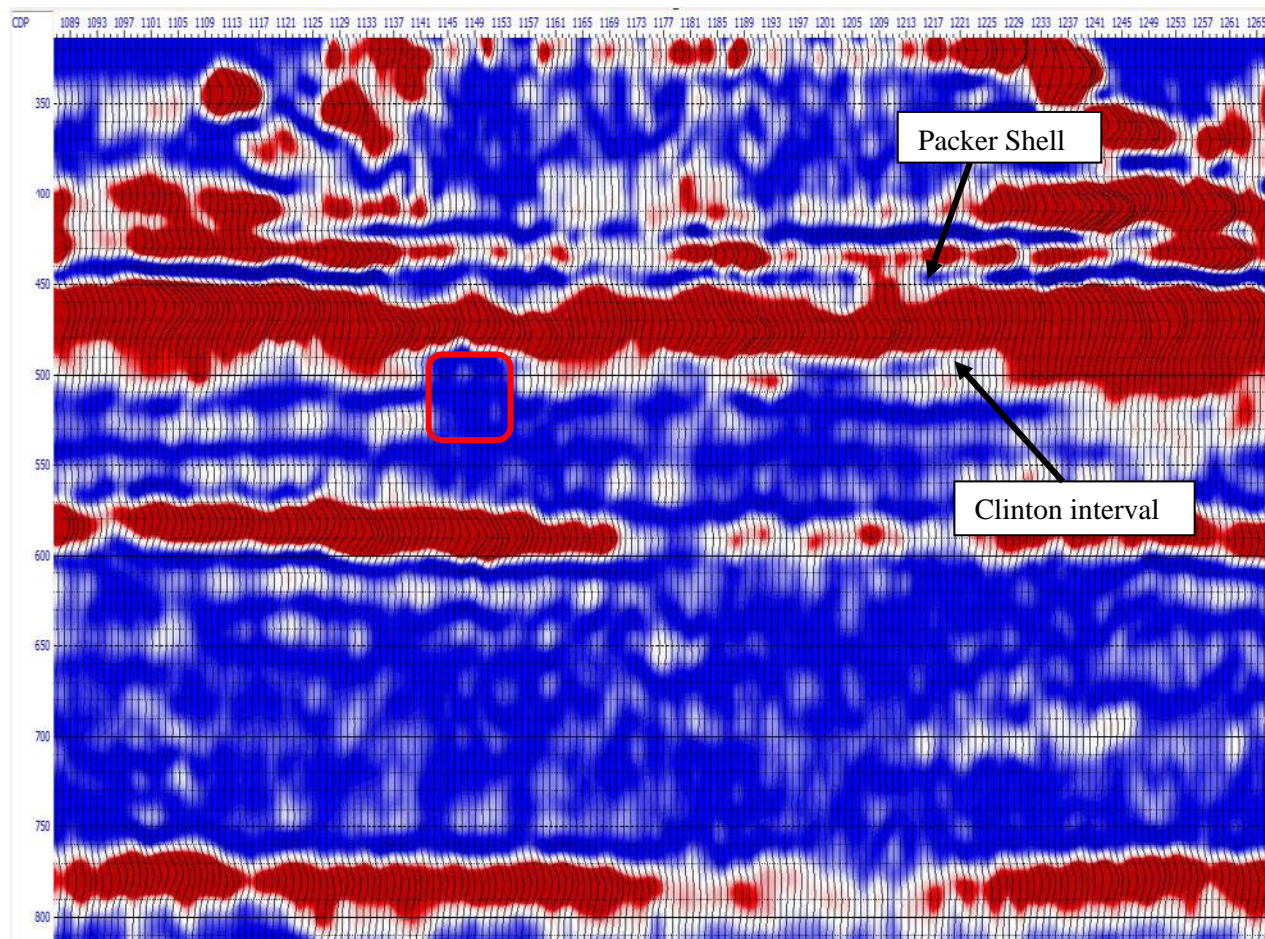


**Figure 22.** A 30 Hz common frequency section of Line3. The red box indicates CDP 1143 to CDP 1161 as the attenuation zone (gas shadow) centered at the top of the Cincinnati Group.

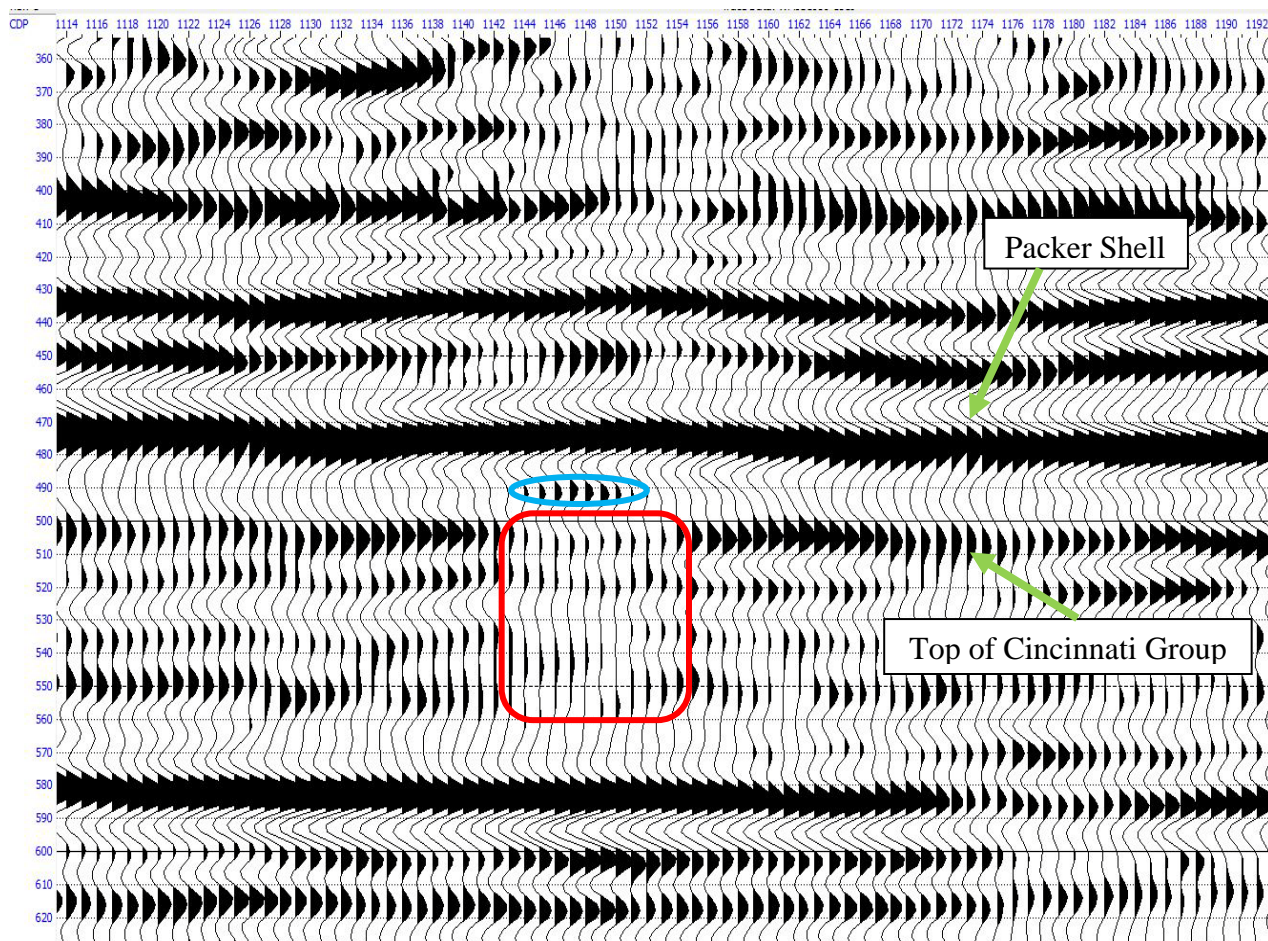


**Figure 23. Gas shadow on Line 3. The Packer Shell and top of the Cincinnati Group are marked. The red box indicates attenuation area at the top of the Cincinnati Group. An anomalous positive reflector is marked with a blue oval.**

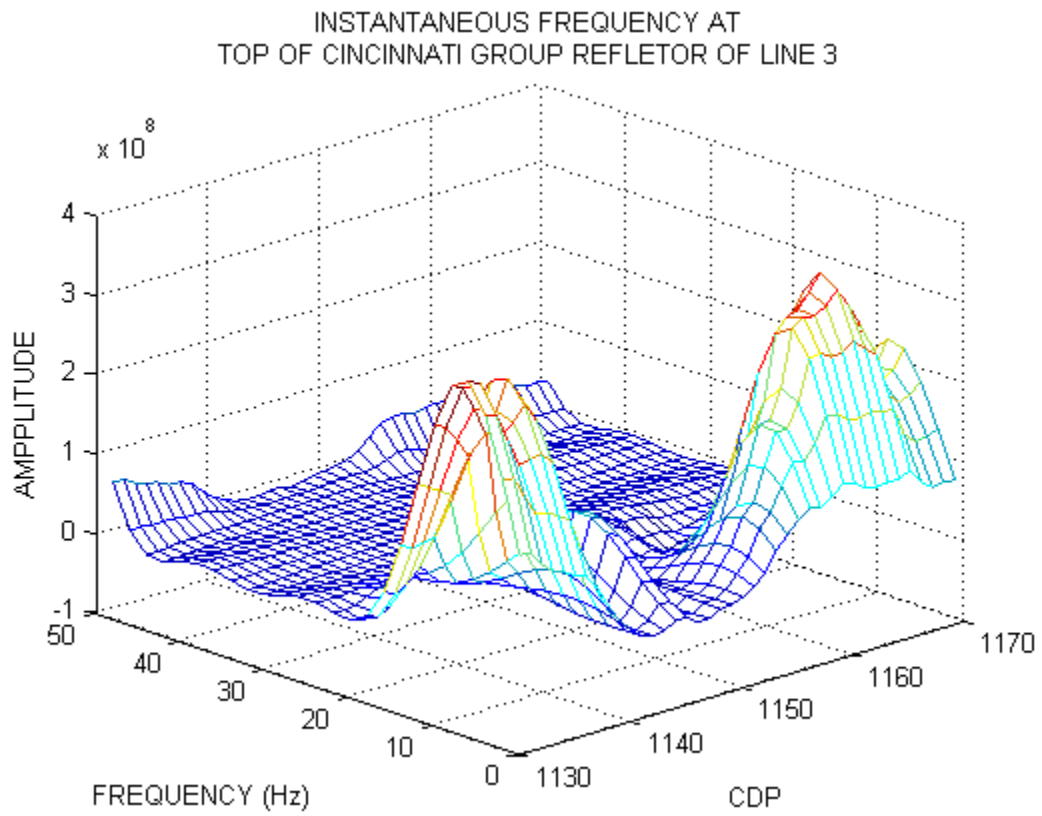


**Figure 24. Instantaneous frequencies at the maximum phase of the reflector corresponding to the top of the Cincinnati Group of Line 3 associated with Figure 23.**



Line 5 had 494 CDPs ranging from CDP 2103 to CDP 2596 and was 5.1 miles long. An apparent gas shadow was found by applying time-frequency analysis as illustrated in Figure 25, Figure 26 and Figure 27 between CDP 2245 to CDP 2265. At 10 Hz a clear attenuation zone beneath the Clinton interval is shown in Figure 25. At 20 Hz (Figure 26), attenuation is still strong within the gas shadow zone. At 30 Hz (Figure 27), the contrast is greater. Figure 28 shows that this gas shadow is also accompanied by an anomalous discontinuous positive reflector immediately beneath the Packer Shell reflector. Figure 29 shows the now familiar behavior with attenuation of all frequencies at the top of the Cincinnati Group within the gas shadow on the seismic section.

Line 6 has 452 CDPs from CDP 2628 to CDP 3079, and is 4.6 miles long. At 10 Hz (Figure 30) time-frequency analysis, a clear attenuation zone is found between CDP 2771 and CDP 2790 as outlined by the red trapezoid. At 20 Hz (Figure 31), however, the attenuation zone has shrunk a little bit, and is found between CDP 2771 to CDP 2782. At 30 Hz (Figure 32) the attenuation zone is even smaller than it was at 20 Hz located between CDP 2772 to CDP 2780. This gas shadow is similar to that displayed in the Gabor gas storage field data in that it does appear to be accompanied by an anomalous discontinuous positive reflector as shown in Figure 33. It is interesting that the attenuation zone became smaller as frequency increased. The top of the Cincinnati Group beneath the Clinton interval is attenuated in a manner similar to other gas shadows in this study as illustrated in Figure 34.

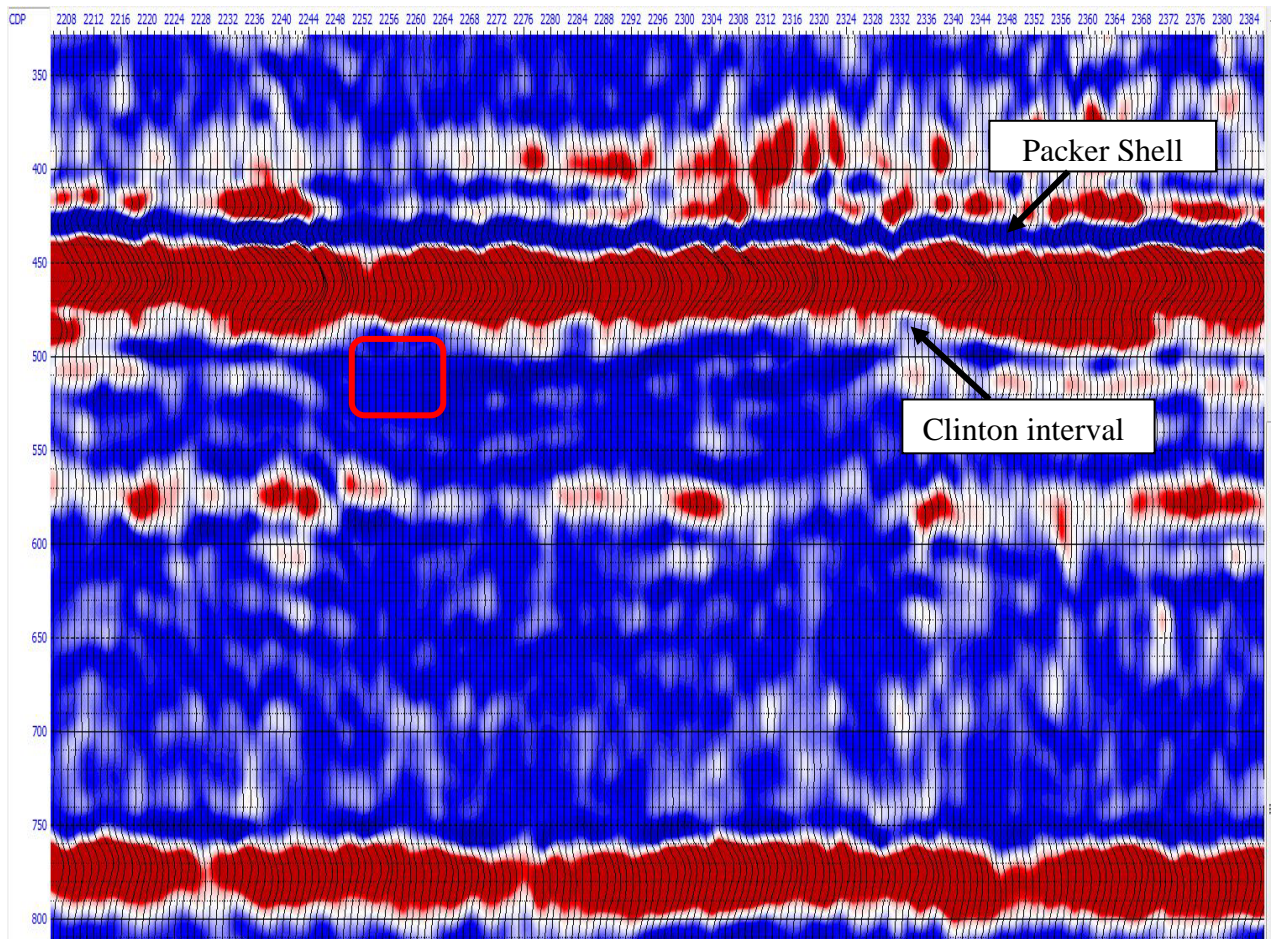


**Figure 25. A 10 Hz common frequency section of Line5. The red box indicates CDP 2245 to CDP 2265 the attenuation zone (gas shadow).**



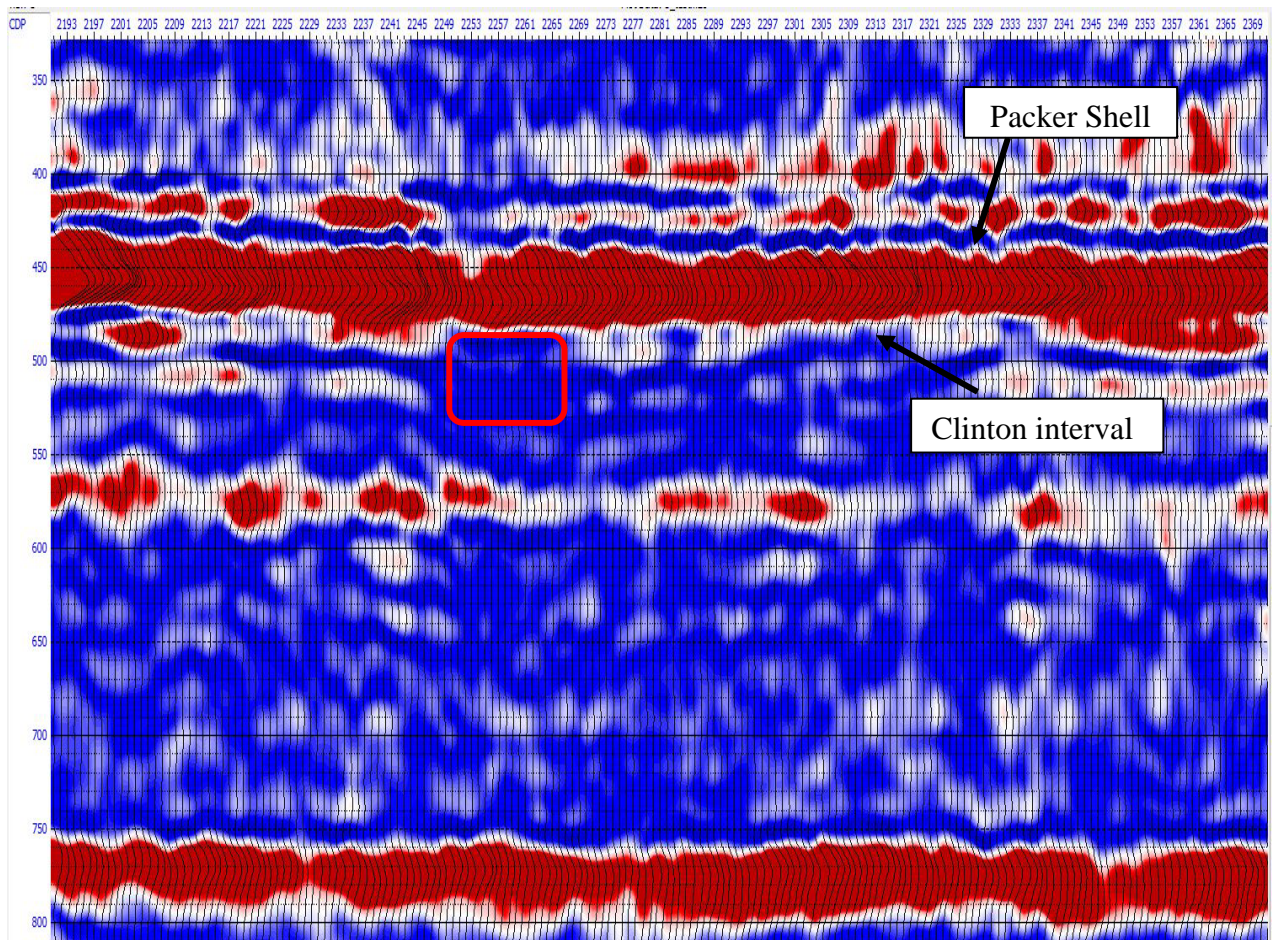


**Figure 26. A 20 Hz common frequency section of Line5. The red Box indicates CDP 2245 to CDP 2265 as the attenuation zone (gas shadow).**



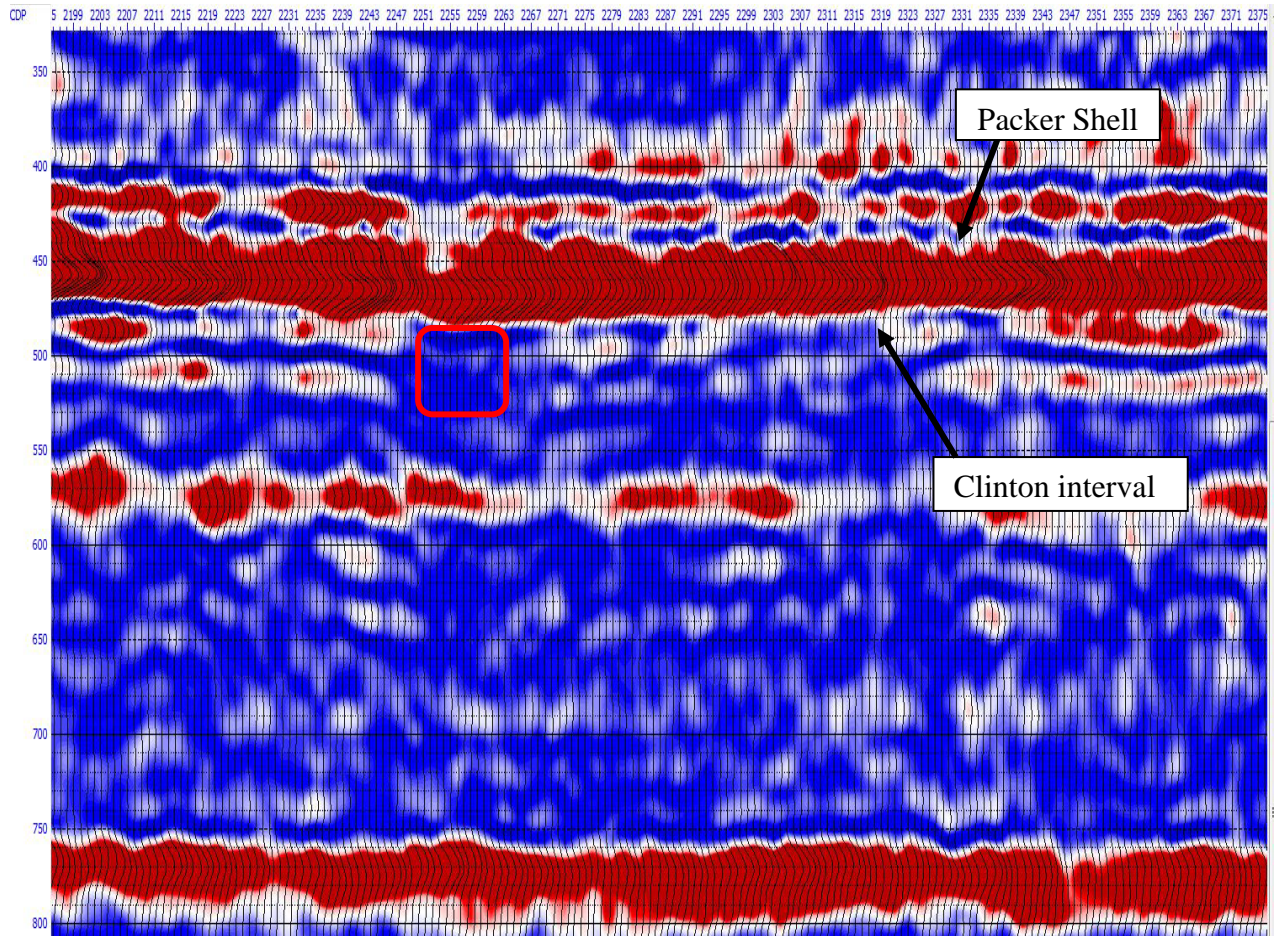


**Figure 27. A 30 Hz common frequency section of Line5. The red box indicates CDP 2245 to CDP 2265 as the attenuation zone (gas shadow).**

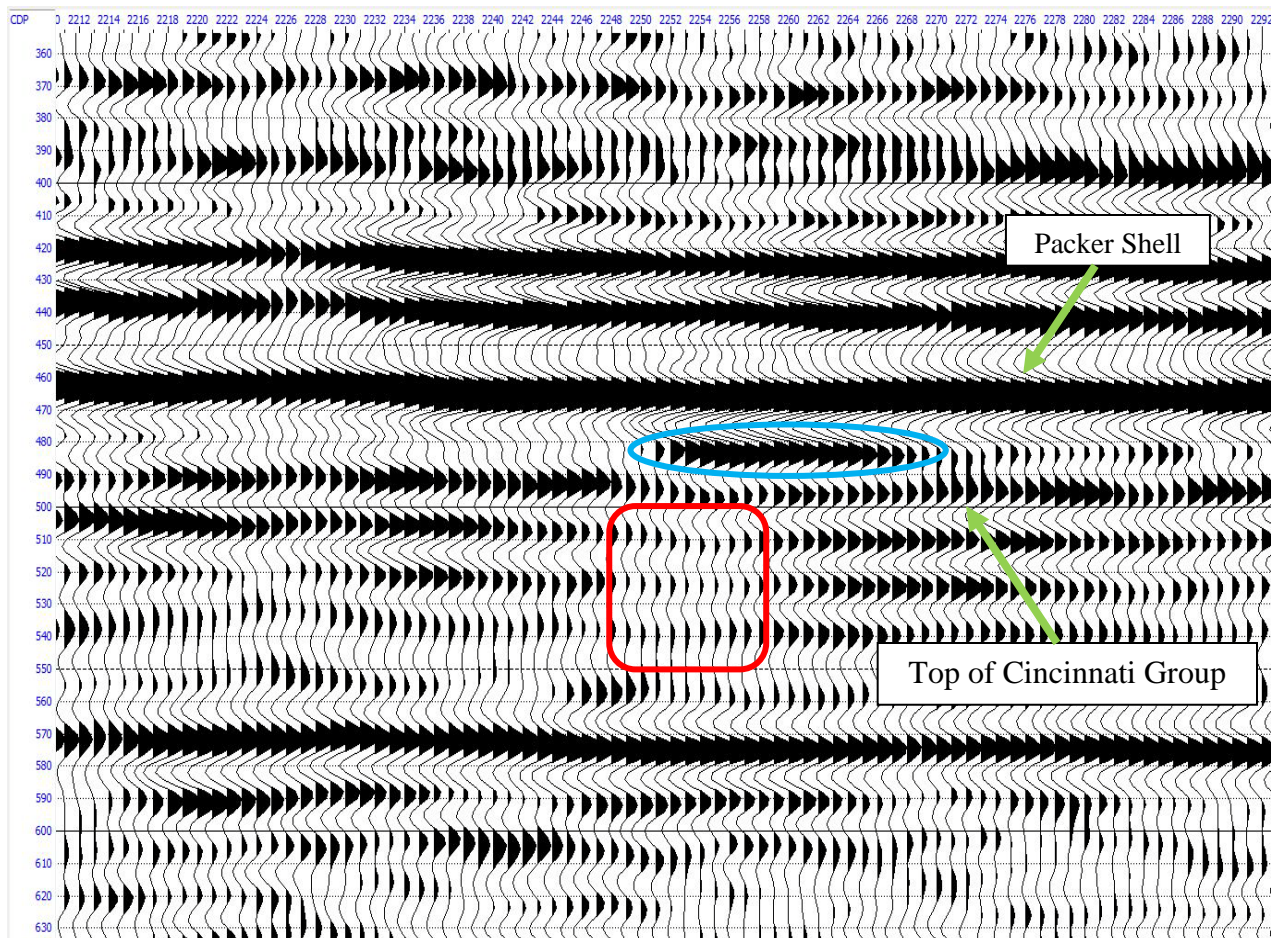


**Figure 28. Gas shadow in Line 5. The Packer Shell and top of the Cincinnati Group are marked. The red box is attenuation area in the top of the Cincinnati Group. An anomalous positive reflector is marked with a blue oval.**

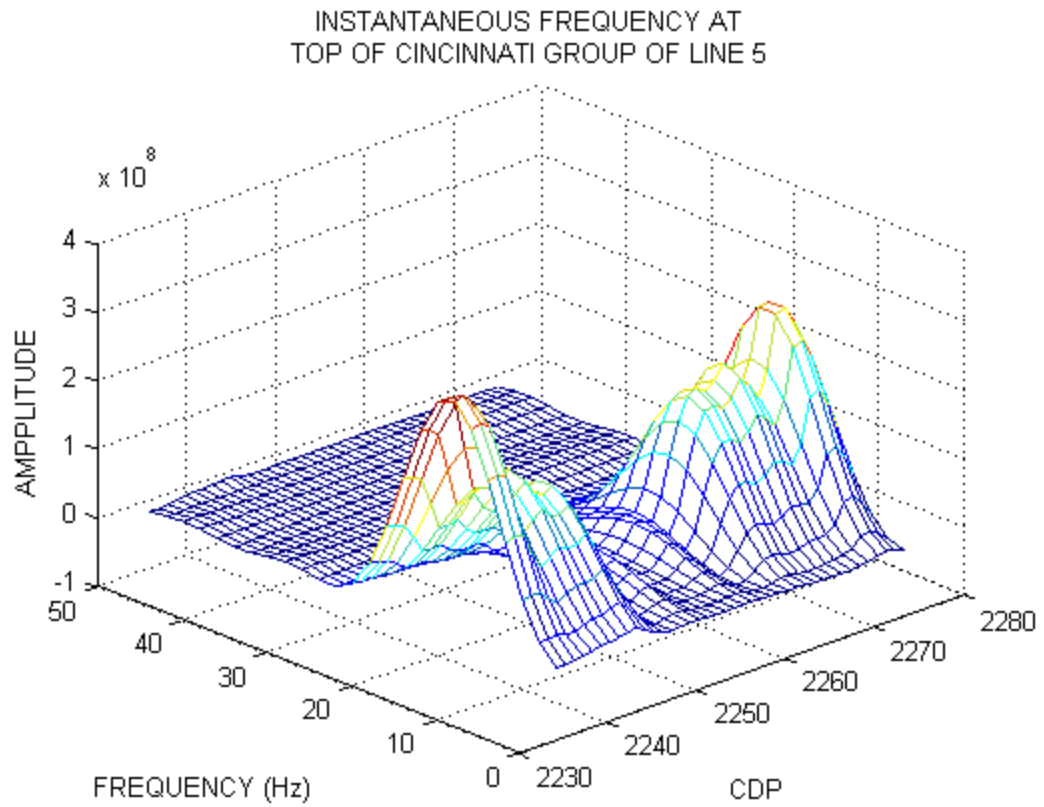


**Figure 29.**Instantaneous frequencies at the maximum phase of the reflector corresponding to the top of the Cincinnati Group of Line 5 associated with Figure 28.



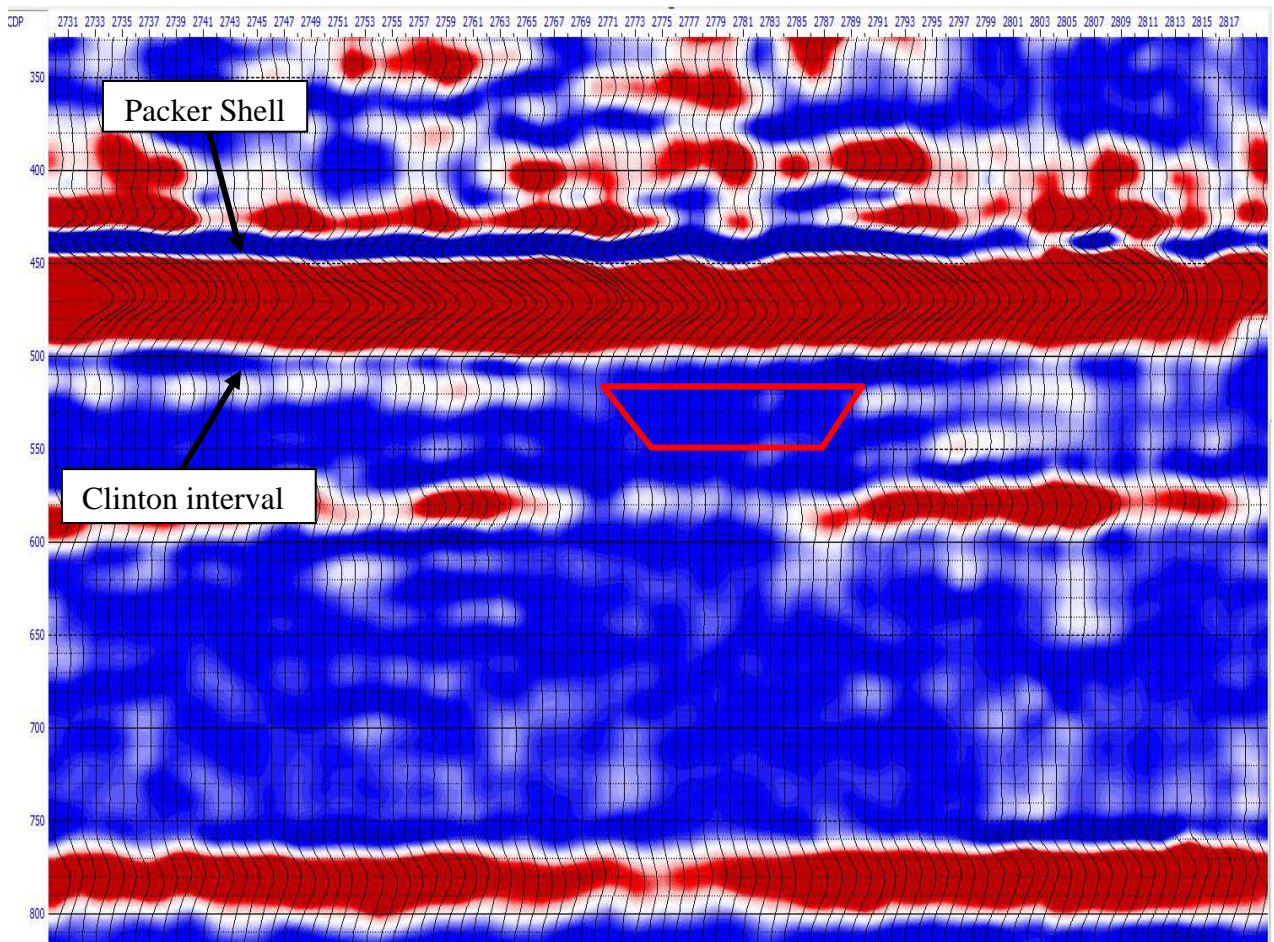


**Figure 30. A 10 Hz common frequency section of Line6. The red trapezoid indicates CDP 2771 and CDP2790 as the attenuation zone (gas shadow).**



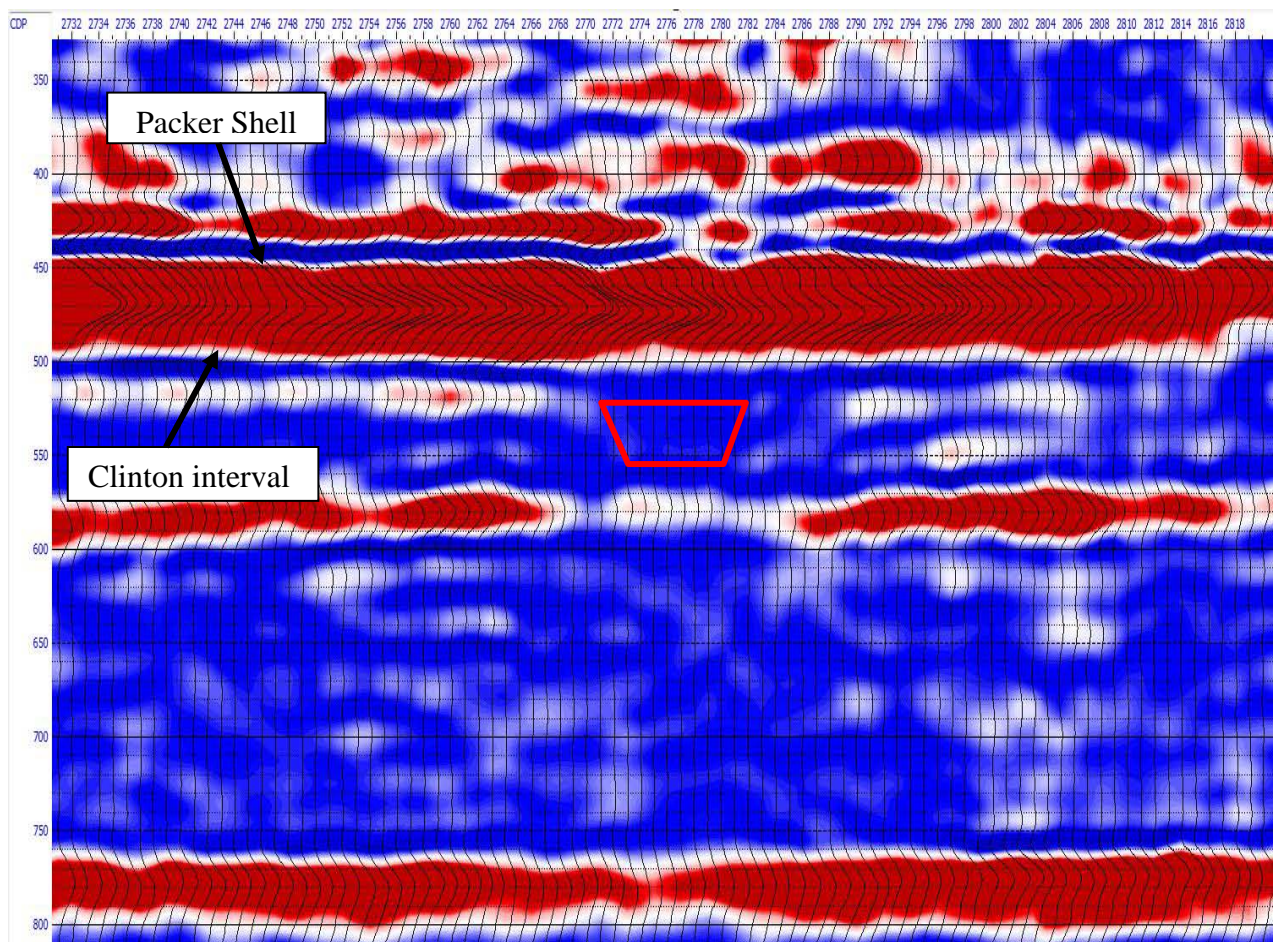


**Figure 31. A 20 Hz common frequency section of Line6. The red trapezoid indicates CDP 2771 to CDP 2782 as the attenuation zone (gas shadow).**



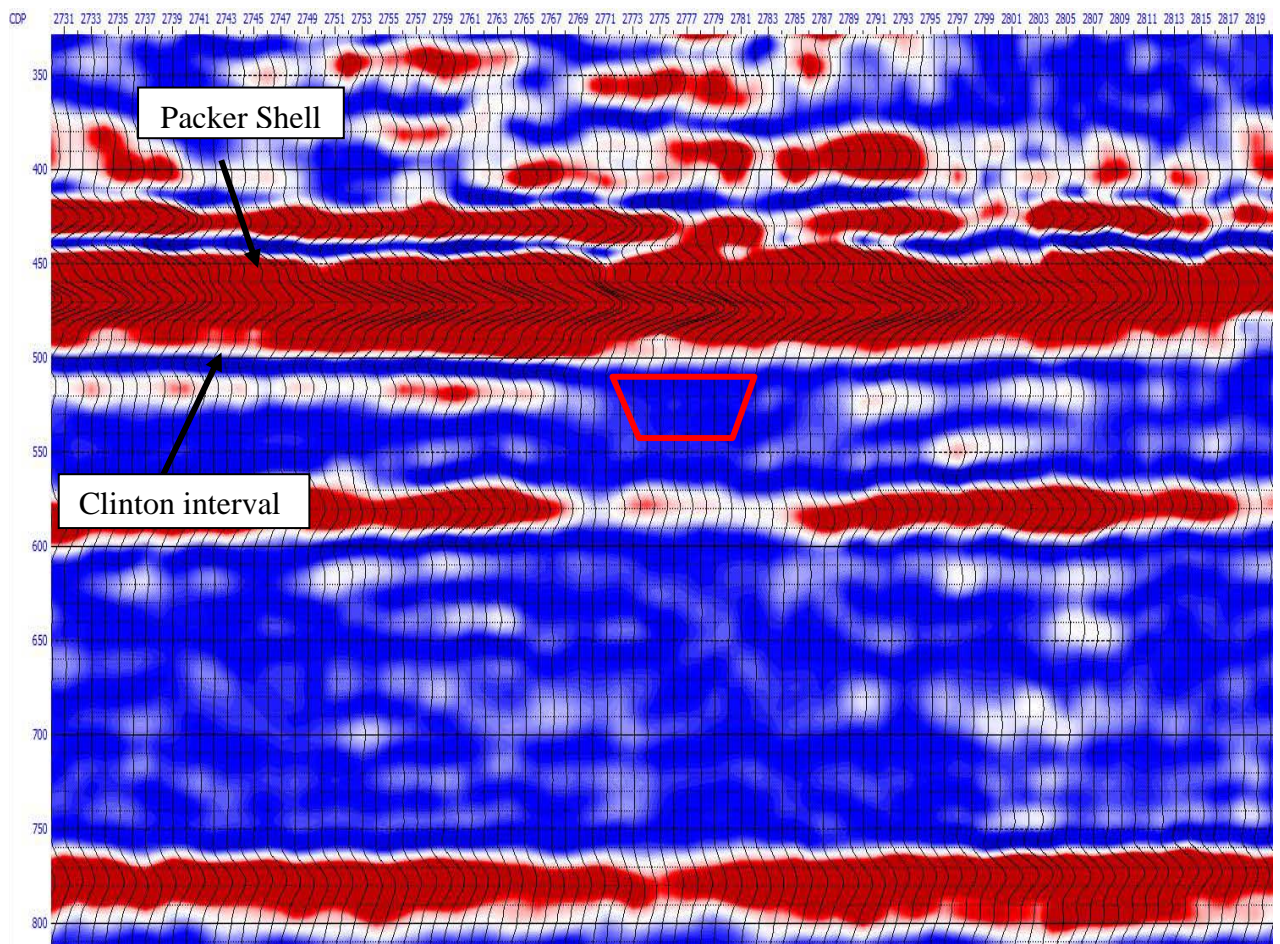


**Figure 32. A 30 Hz common frequency section of Line6. The red trapezoid indicates CDP 2272 to CDP 2280 as the attenuation zone (gas shadow).**



**Figure 33. Gas shadow in Line 6. The Packer Shell and top of the Cincinnati Group are marked. The red trapezoid indicates attenuation area at the top of the Cincinnati Group reflector.**

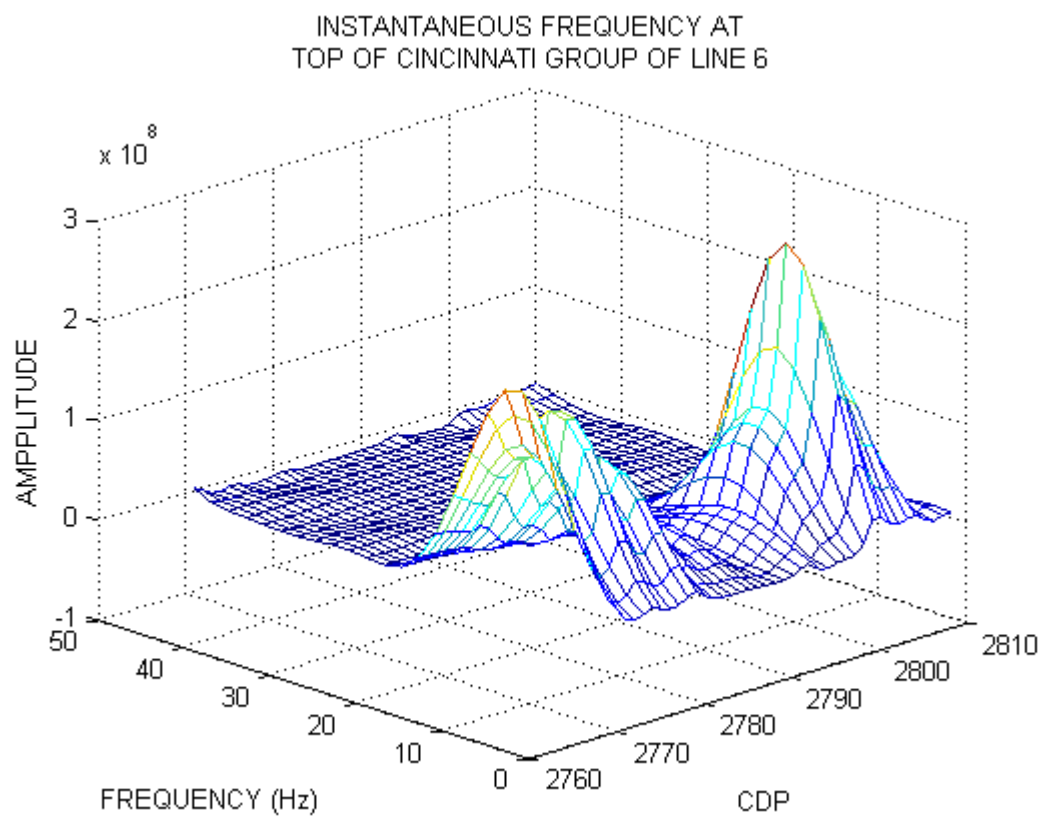


**Figure 34. Instantaneous frequencies at the maximum phase of the reflector corresponding to the top of the Cincinnati Group of Line 5 associated with Figure 33.**

The results of time-frequency analysis are compared to the Initial Production map in Figure 35 of the Clinton gas wells in Muskingum County. Four possible gas shadows were identified at CDP 195-205 in Line 1, CDP 1143-1161 in Line 3, CDP 2245-2265 in Line 5 and CDP 2271-2278 in Line 69. These are represented as red ovals in Figure 35. There appears to be no strong correlation between gas shadows and the high initial production zone illustrated. Gas shadows on Lines 5 and 6 appear in the area with higher natural gas initial production, while gas shadows in Lines 1 and 3 have no apparent connection with production. No gas shadows are observed within the southern portion of the seismic data.



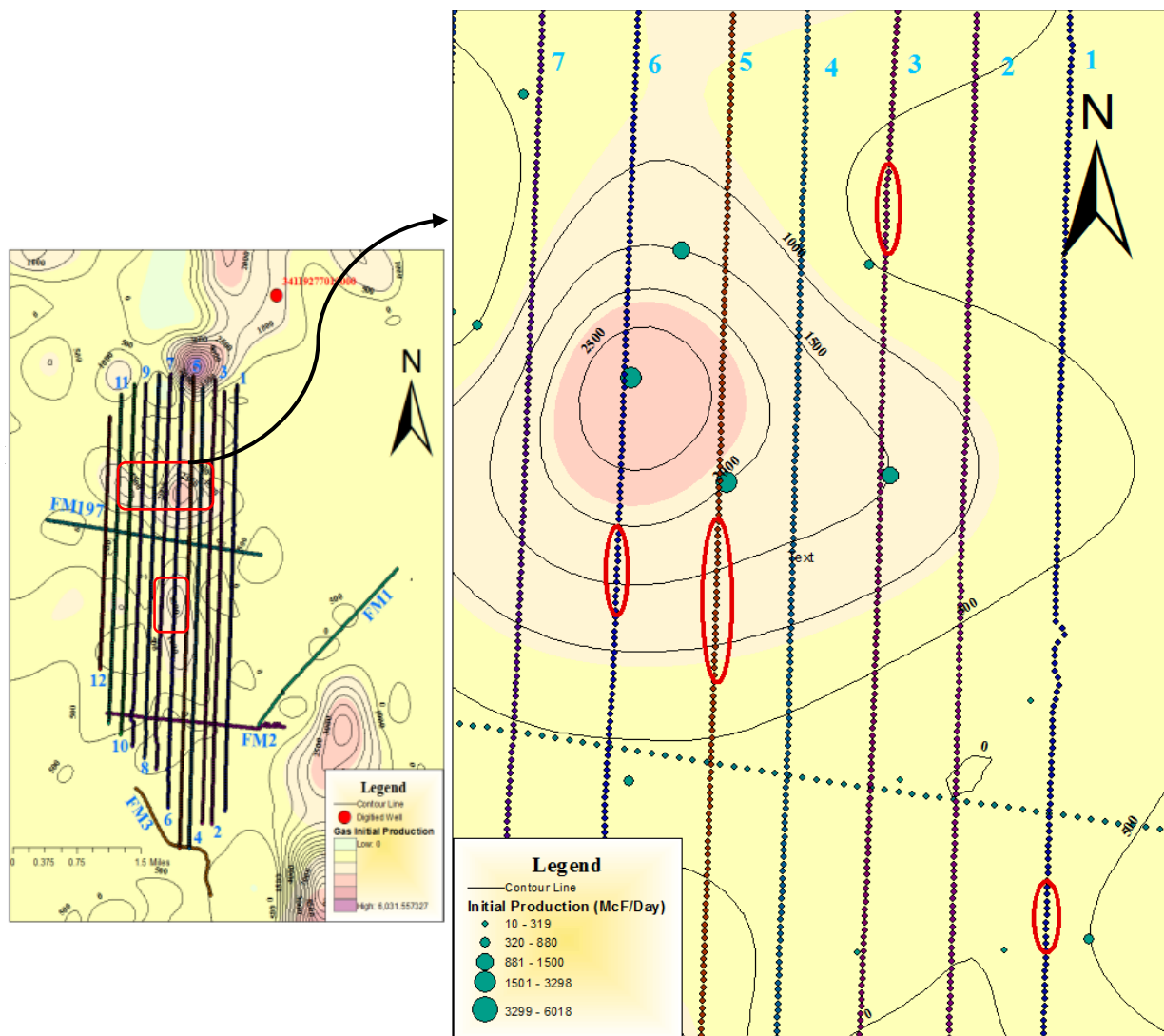


**Figure 35. High initial gas production zones with observed gas shadows marked with red ovals.**

## 5 Summary & Discussion

I applied instantaneous frequency analysis using the Smoothed Pseudo Wigner-Ville Distribution to 2D land seismic reflection data from the Gabor Dominion East Ohio gas storage field and to seismic reflection data from Muskingum County, Ohio. The data from the Gabor storage field contained previously identified gas shadows beneath the fully charged Clinton interval. The Muskingum County data were acquired in the vicinity of high Clinton gas production and possible gas shadows beneath the Clinton interval were identified in this area. Reflectors on the Muskingum County data were identified on these sections using velocity and density logs from a nearby deep well to calculate reflectivity coefficients. A source wavelet was extracted from the data and convolved with the reflectivity. The results showed the gas shadows in Ohio are different from low frequency shadows previously reported in seismic reflection data. Rather than enhancement of low frequencies and attenuation of high frequencies in as reported in areas such as the Gulf of Mexico, all frequencies appear to be equally attenuated. Otherwise continuous reflectors that pass through gas shadow beneath the fully charged Clinton interval virtually disappeared.

There is no accepted explanation of gas shadows in seismic reflection data. Previously, gas shadows and other direct indicators of hydrocarbons were reported from relatively young Cenozoic and Mesozoic basins with very high porosity and permeability in loosely cemented sediments. The effects reported here are from well cemented Paleozoic reservoirs that often have reduced porosity due to a long history diagenesis.

Contours of natural gas initial production were produced using data from Clinton wells in the vicinity to get a rough idea of reservoir quality. Potential gas shadows were identified using instantaneous frequency analysis on the seismic data two shadows were found to be in the vicinity of high initial production wells. Using initial production is only a way to gain a rough characterization of the reservoir quality of the Clinton interval which is highly variable due to variations in porosity. Furthermore, the seismic data were acquired after the wells produced and consequently a depleted reservoir may have no effect on the seismic data. Unfortunately, the available well log data are not of sufficient quantity to conduct any meaningful reservoir analysis.

In portions of the data from Muskingum County positive reflectors were found to develop immediately above the gas shadow zones as indicated by the blue ovals in Figure 18, Figure 23 and Figure 28. Since three out of the four gas shadow found on these lines show this interested feature, I suggest that these reflectors might well have a connection with the gas shadows. They appear at the Clinton interval and may be the result of thickening of the hydrocarbon-related Clinton sandstone bodies. The presence of hydrocarbon might also be related to the appearance of these events. However, this feature does not appear in the Gabor gas storage field data. The hydrocarbon bearing sandstones in the Clinton interval are discontinuous throughout eastern Ohio. The thickness or lateral extend of the Clinton sandstones varies rapidly in these fluvial deltaic deposits. The presence of natural gas may affect the acoustical properties of sediments. The gas storage field was fully charged when the seismic data were acquired, likely at pressures that are higher than normal in natural reservoirs, and this may have contributed to the gas shadow effect. Further observation of subtle seismic reflection features in other

data acquired over Clinton gas reservoirs are required to confirm a correlation of gas shadows with the development reflectors of limited extend at this particular interval. Ohio gas shadows are only revealed if a continuous reflector is found immediately beneath the Clinton interval. As an exploration tool, it is important that target reservoirs be appropriately located on the seismic section.

In this study I only used the Smoothed Pseudo Wigner-Ville distribution to analyze the spectral variations in known and potential gas shadows produced by natural gas in the Clinton interval. There are in fact many ways to conduct time-frequency analysis and further work is needed to quantify which particular method may be the best. The Smoothed Pseudo Wigner-Ville distribution does seem a robust method for this application. Application to 3D data may also be valuable to produce distributions of these attributes on a mapped surface.



## 6 References

- BEY, S. (2011). Reservoir Characterization and Seismic Expression of the Clinton Interval over Dominion's Gabor Gas Storage Field in North-East Ohio. Master of Science Thesis. *Wright State University*.
- BOASHASH, B., WHITEHOUSE, H.J. (1986). Seismic Application of the Wigner-Ville Distribution. *IEEE Int.Conf. Systems and Circuits*. P 34-37.
- BROWN, L.F. (1979). Lithofacies Map of Lower Silurian Deposition in Central and Eastern United States and Canada. *American Association of Petroleum Geologists Bull.* V. 39. P. 60-74.
- EBROM, A.R. (1996). Seismic Attributes and Their Classification. *The Leading Edge*. October. P. 1090.
- CASTAGNA, J. P., SHENGJIE, S., SEIGFIED, R. W. (2003). Instantaneous Spectral Analysis: Detection of Low-Frequency Shadow Associated with Hydrocarbon. *The Leading Edge*. February.
- COLEMAN, J. A., PRIOR, D. P.(1980). Deltaic Sand Bodies. *AAPG Continuing Education Course Note Series*. No. 15. 171 p.
- FLANDRIN, P. Time-Frequency/Time-Scale. (1999). *Academic Press, San Diego*.
- HANEBERG-DIGGS, D. (2014). Seismic Attributes of the Clinton Interval Reservoir in the Dominion East Ohio Gabor Gas Storage Field Near North Canton. Master of Science Thesis. *Wright State University*.
- KNIGHT, W. V. (1969). Historical and Economic Geology of Lower Silurian Clinton Sandstone of Northeastern Ohio. *Petroleum Geologists Bull.* 53(7). P. 1421-1452.
- KELTCH, B. (1985). Why Use Geology for Clinton Exploration? (Examples and Reasons from Guernsey County Ohio. *Consolidated Resources of America, Inc.*
- MARFURT, K.J., CHOPRA, S. (2005). Seismic Attributes for Prospect Identification and Reservoir Characterization. *SEG Geophysical Developments Series* No. 11.
- MIKAN, F. W. (1973). Paleoenvironmental Interpretation of the Lower Silurian "Clinton sands" in Guernsey County Ohio. Master Thesis of Science. *The Ohio State University*.
- PEPPER, J. F., DEWITT, W., EVERHART, G.M. (1953). The Clinton Sands in Canton, Dover Massillon, and Navarre Quadrangles, Ohio. Oil and Gas Geology of the Clinton Sands of Ohio. *U.S. geological Survey Bulletin* 1003-A

- QIAN, S.,CHEN, D. (1996). Joint Time-Frequency Analysis: Method and Application, Prentice Hall.
- ROSHAN-GIAS, A.,SHAMSOLLAHO, M.B.,MOBED, M., BEHZAD, M. (2007). Estimation of modal parameters using bilinear joint time-frequency distributions. *Mechanical Systems and Signal Processing*. 21. P. 2125-2136.
- SHANNON, H.G.,DAHL, A.R. (1971). Deltaic Stratigraphic Traps in West Tuscola Field Taylor County, Texas. *America Association of Petroleum Geologist Bull.* V. 55. P. 1194-1205.
- SWANSON, D. C. (1979). Deltaic Deposits in the Pennsylvanian Upper Morrow Formation of the Anadarko Basin in Hyne, Pennsylvanian Sandstones of the Mid-Continent. *Tusla Geologic Society. Spec.* P. 360
- SANTINDER,C., KURT, J.M. (2005). Seismic Attributes for Prospect Identification and Reservoir Characterization. *SEG Geophysical Developments Series* No. 11.
- SHADRACH, R. J., (1989). Subsurface geology of the Clinton section (Lower Silurian Albion Group) in Medina County, Ohio, Master of Science Thesis, *Kent State University*.
- TANER M.T., KOEHLER,F., SHERIFF,R.E. (1979). Complex Seismic Trace Analysis. *Geophysics*. 44 (6). P. 1041-1063.
- VILLE, J. (1948). Theorit et applications de la notion de signal analytique. *Cable Transmission* 2A. P. 61-74.
- VISHER, G. S. (1965). Use of Vertical Profile in Environmental Reconstruction. *America Association of Petroleum Geologists Bull.* 49(1). P. 41-61.
- WILSON, J. T. (1988). Portage County, Revisited: An Analysis of the Occurrence of Oil and Gas in the Lower Silurian “Clinton” Sandstone Reservoir in Portage County, Ohio. Master Thesis of Science. *Kent State University*.
- WU, X.; LIU, T. (2009). Spectral decomposition of seismic data with reassigned smoothed pseudo Wigner-Ville distribution. *Journal of Applied geophysics*. P 386-393.
- WYTOVICH, D, A. (2010). Reservoir Analysis of the Interval in Stark and Summit Counties, Ohio. Master of Science Thesis. *Wright State University*.